RADIOLOGY STUDY

RADIOLOGY STUDY

DEAR FRIENDS AND COLLEAGUES!

We are glad to present the first issue of our journal in a completely new format. In this issue, a large number of articles and interesting cases from practice dedicated on different radiologic sub-specialisation.

We believe that readers will find in this issue materials that will answer their questions and help in practical work. We are waiting for your letters with questions and suggestions on the subject of the following issues.

СОДЕРЖАНИЕ

CONTENTS

SCIENCE PART

Methods for assessing the dependence of ADC on temperature with DWI MRI

D.S. Semenov, K.A. Sergunova, E.S. Akhmad, Yu.A. Vasilev.
Practical and Clinical Research Center of Diagnostics and Telemedical Technologies, Department of Health Care of Moscow

Purpose of the study

The purpose of this study is to develop a methodology for assessing the temperature dependence of the measured diffusion coefficient (ICD), calculated when performing diffusion-weighted magnetic resonance imaging (MRI).

Materials and methods

To create different ICDs, physical models of obstructed diffusion were used, which are aqueous solutions of the polymer (polyvinylpyrrolidone) with different concentrations. The temperature of the solutions was measured using a fiber optic temperature measurement system with sensors fixed inside the tubes. The dependence of the change in ICD on temperature was recorded when the EPI sequence was periodically started while the phantom was cooling from 38 °C to 22 °C.

Results

As a result of an experimental study, ICD temperature dependences were obtained for each model of diffusion obstructed. Approbation of the technique showed that in the temperature range allowed in the MRI room by the current regulatory documentation (20-23 °C), the values of ICDs can differ by up to 25 %. Calculated approximating coefficients of the dependence of ICD on temperature for the used PVP solutions.

Conclusion

The presented experimental technique allows to increase the efficiency of the procedure of periodic quality control using a phantom for diffusion-weighted magnetic resonance imaging by introducing a correction factor.

Keywords:

diffusion-weighted magnetic resonance imaging, apparent diffusion coefficient, quality control

Semenov Dmitry Sergeevich
Phone number: +7 (916) 339-76-83
E-mail: d.semenov@npcmr.ru

Introduction

Diffusion-weighted magnetic resonance imaging (DWI MRI) is one of the methods of medical visualization applied for detection and assessment of neoplasms. Apparent diffusion coefficient (ADC), a quantitative parameter which reflects the movement of water molecules within tissue, is a specific feature of this mode. The use of ADC values in order to form the conclusion about the probable malignancy of the tumor [1, 2] necessitates controlling of the accuracy and repeatability of this indicator measurement [3].

Traditionally, image quality control in radiology involves the use of phantoms – special test objects with known properties. Obtained phantom images allow to judge about the correct operation of the equipment and to decide whether this equipment should be further used and if there is a need for correction factor.

The accuracy of ADC measurement depends on such factors as the gradient calibration accuracy and gradient amplitude. The direct control of these two parameters is difficult so a phantom was developed [4]. The phantom allows to simulate the entire range of self-diffusion coefficients recorded in organ tissue including different types of diffusion (limited, difficult, and unlimited) [5] and as a result to improve the accuracy of ADC measurement with correction factor. Comparison of different devices confirms the difference in ADC values determined not only on the equipment of different manufacturers, but also on tomographs of the same model located in different medical institutions [6], and therefore confirms the need of introducing control methods and equipment cross-calibration in practice.

The next step is to investigate the influence of sample temperature on the recorded ADC values in addition to the above mentioned factors contributing to ADC measurement. Temperature fluctuation are generally explained by the variable air temperature in the MRI treatment room (20–23 °C according to SanRaN 2.1.3.2630-10 [7]), tomograph and climate control unit hearth heat.

Thus, the main purpose of the study is to develop method of assessing the dependence of ADC samples on temperature.

Materials and methods

The Einstein-Smoluchowski equation is the most famous equation to represent the dependence of self-diffusion coefficient on temperature:

$$D = \frac{kT}{3\pi\eta d},$$ (1)

where η – viscosity, d – particle size, k – Boltzmann's constant, T – absolute temperature.

However, only estimated values can be obtained when applying the equation for this problem due to macroscopic approximations used for this equation (1) limit its application. Therefore, the Einstein-Smoluchowski equation was used only for evaluative calculations while selecting materials for the phantom. This work offers a method of experimental determination of the dependence of ADC on temperature.

Aqueous solutions of the polyvinylpyrrolidone (PVP) with different concentrations (0 (water), 10, 30, 50, 70 %) were used for modeling obstructed diffusion resulting from the collisions between water molecules and macromolecules, cell organelles, and compartments. Tubes with this solutions were placed on a special frame in nonmagnetic plastic container filled with water.

According to IEC 60601-2-33:2010 [8] it is prohibited to conduct MRI if the local body temperature exceeds 39 °C. A preheat of the phantom and conducting MRI in (DW) MRI mode while the phantom cools down appeared to be the rational decision.

Accurate measurement of solutions temperature in the phantom is also challenging. The following methods are traditionally used for this purpose: MR-termometry, non-contact measurements (e.g. thermography), measurements with contact sensors. The experience in this kind of studies showed that it is preferable to use fiber-optic temperature sensors that are resistant to magnetic fields and have high accuracy (up to 0.01 °C) [9]. In addition, the response time of the sensors is negligibly short compared to the scanning time, which makes is possible to assess the correctness of the data used.

The control unit of multichannel fiber-optic system of deformation and temperature measurement "ASID-12" manufactured by Optiz-Monitoring Ltd. (figure 1) was located in the MRI technical room. The sensors were led through a technological hole in the Faraday cage and fixed in the test tunes centers. An alcohol thermometer was used to monitor fiber-optic system measurements.

Picture 1. *The control unit of fiber-optic system for temperature measurement*

In order to ensure a gradual temperature change before the study the phantom was thermostatted by placing it into flowing water with temperature of 38.0 °C. Air temperature in the MRI treatment room was – 23,0 °C.

Scanning was performed on Toshiba Excelart Vantage 1,5 T using DWI_EPI pulse sequence with the following parameters: TR 5300 ms, TE 100 ms, FOV 26 x 26 sm, matrix 128 x 128, slice number 15, b-value = 600, 800 s/mm2, scanning time 32 s. The scanning was started with the following frequency: 38 – 34 °C – every minute, 34 – 30 °C – every 2 minutes, 30 – 28 °C – start every 5 minutes.

The statistical analysis of the received ADC maps data was carried out as follows:

- with the help of developed software the regions of interest covering about 80 % of sample cross-section area for each tube (ROIj) were identified in the MR-images;

- the calculation of the average value of ADC Dj and the standard deviation σj was performed in the automatic mode on the sample Di,j, i = 1, 2 … Nj, where Nj is the number of pixels within the ROIj;

- pixels selected erroneously and corresponding to the condition (2) were excluded from the obtained sample.

$$D_{ij} \notin \left(D_j - 3\sigma_j, D_j - 3\sigma_j \right); \quad (2)$$

At the same time, the average temperature value, obtained from the sensors during the study, was taken as true temperature value.

Results

Picture 2 shows the dependence of ADC solutions of the phantom on temperature obtained as a result of the proposed method.
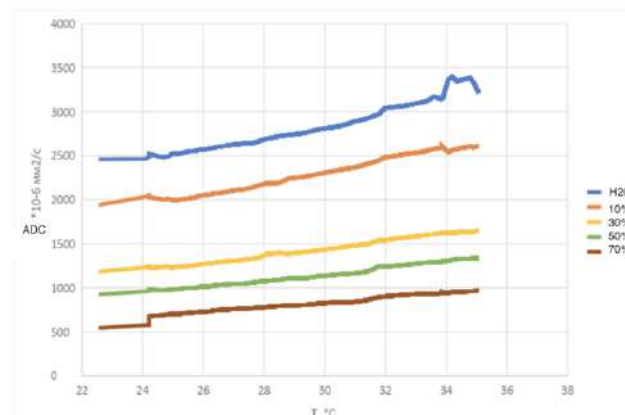
Picture 2. *The temperature dependency graph fo ADC for different PVP concentrations*

Testing of the technique showed that within the temperature range allowed by the current regulatory documentation, registered ADC values may vary up to 25 %. The study of the dependence of ADC on temperature allowed to conduct approximation curves and calculate their coefficients.The closest linear function for the PVP solutions with concentrations of 50 % and 70 % was y = a*x + b. Coefficients a and b are determined using the least squares method. Table 1 shows the calculated coefficients.

The dependence of ADC on temperature has a quadratic function y = c*x2 + a*x + b for aqueous PVP solutions with concentrations of 0, 10, and 30 %.

Table 1. *Approximating coefficients for the dependence of ADC on temperature for specified water PVP solutions*

	PVP 50 %	PVP 70 %	PVP 0 %	PVP 10 %	PVP 30 %
c	0	0	4.73	1.49	0.71
a	35.55	89.90	-199.49	-26.96	-0.73
b	29.63	-59.68	4550.10	1776.50	816.25

The use of calculated approximating coefficients allows to correct ADC measurements performed under different temperature conditions and to conduct comparative tests to compare the results obtained from different tomographs.

A peak of water diffusion coefficient values at 34

– 35 °C may be due to the fluid movements inside the phantom caused by its movements with the patient table during initial positioning.

High accuracy and repeatability of ADC measurement at (DW) MRI is the result of this method.
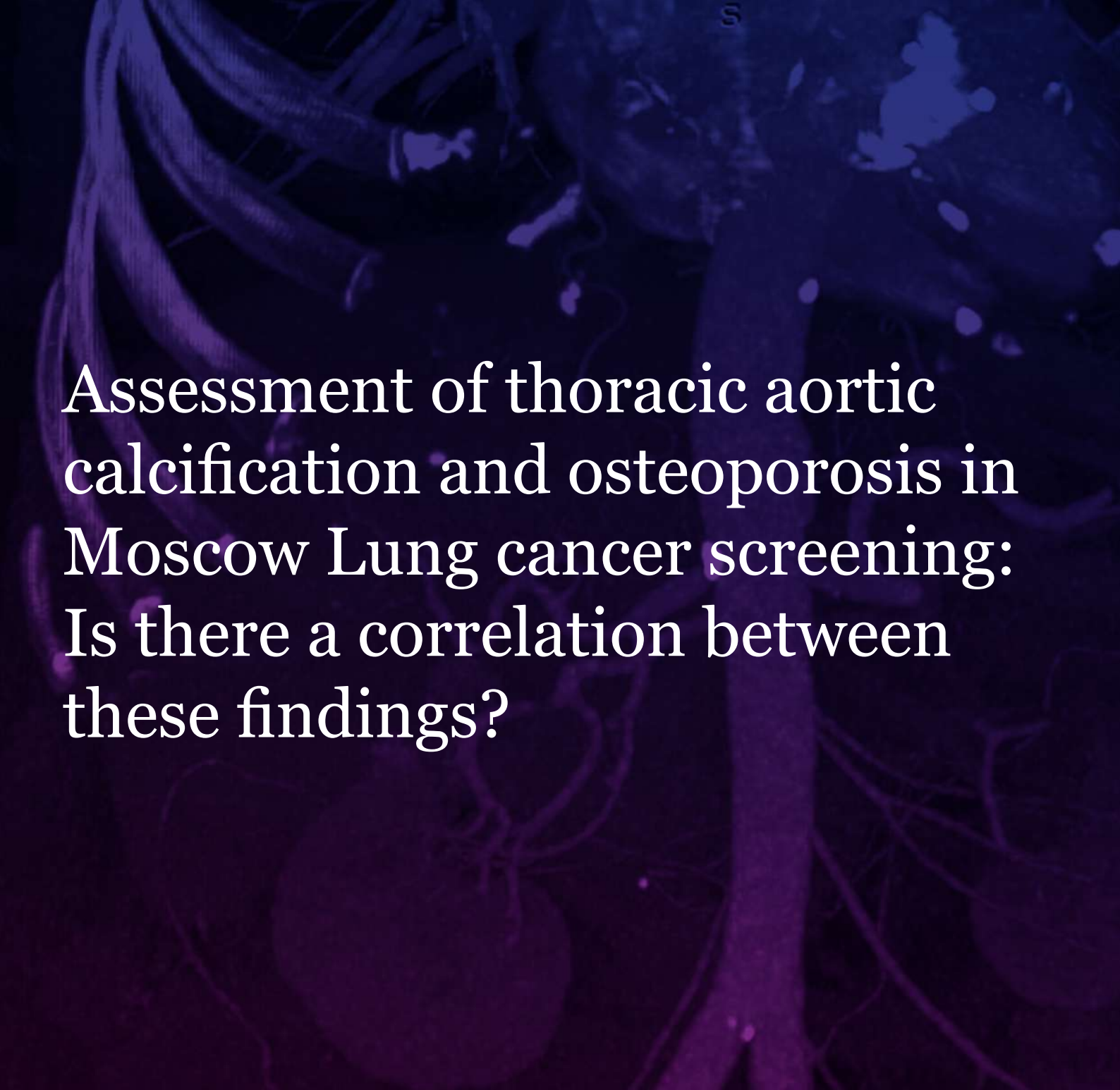
Conclusion

This work has shown the possibility and timeliness of assessing the dependence of ADC on temperature using (DW) MRI to ensure the quality of performed MR-studies. The presented experimental method allows to increase the efficacy of periodic quality control procedure with the use fo phantom for diffusion-weighted magnetic resonance imaging by introducing a correction factor.

The results of this work can also be used while developing recommendations for ADC measurement for diagnostic purposes.

References:

1. Bickel H., Pinker-Domenig K., Bogner W., Spick C., Bagó-Horváth Z., Weber M., et al. Quantitative apparent diffusion coefficient as a noninvasive imaging biomarker for the differentiation of invasive breast cancer and ductal carcinoma in situ. Invest Radiol. 2015; 50 (2): 95-100.

2. Gawande R.S., Gonzalez G., Messing S., Khurana A., Daldrup-Link H.E. Role of diffusion-weighted imaging in differentiating benign and malignant pediatric abdominal tumors. Pediatr Radiol. 2013; 43 (7): 836-845.

3. Sergunova К. А., Karpov I. N., Gromov A. I., Morozov A.K., Semenov D.S. Development of a quality assurance phantom and software module for comparative assessment of neoplastic processes in diffusion-weighted magnetic resonance imaging and diffusion-weighted imaging with background suppression. Biotekhnosfera. 2016; 5 (47): 9-13. (in Russian).

4. Sergunova К. А., Petraikin A.V., Semenov D.S., Akhmad E.S. Phantom device for monitoring parameters of diffusion-weighted images of magnetic resonance imaging. Patent RF no. 187202, G 01 N 24/08, 2019. (in Russian).

5. Sergunova K. A., Petraikin A.V., Akhmad E.S., Kivasev S.A., Semenov D.S. et al. Modeling Diffusion Processes in Magnetic Resonance Imaging. Radiology - Practice. 2019; 2 (74): 50–68 (in press). (in Russian).

6. Kivrak A.S., Paksoy Y., Erol C., Koplay M., Ozbek S., Kara F. Comparison of apparent diffusion coefficient values among different MRI platforms: a multicenter phantom study. Diagnostic Interv Radiol. 2013; 19 (6): 433-437.

7. SanPiN 2.1.3.2630-10 'Sanitary and epidemiological requirements for organizations engaged in medical activities' (as amended on June 10, 2016). 2010. (in Russian).

8. IEC 60601-2-33:2010 Medical electrical equipment - Part 2-33: Particular requirements for the basic safety and essential performance of magnetic resonance equipment for medical diagnosis. Moscow, Standartinform Publ., 2016, 86 p. (in Russian).

9. Vasilev Y.A., Semenov D.S., Yatseev V.A., Akhmad E.S., Petraikin A.V., Marusina M.Y., et al. Experimental study of ferromagnetic objects heating during magnetic resonance imaging. Sci Tech J Inf Technol Mech Opt. 2019; 19 (1): 173-179. (in Russian).

Assessment of thoracic aortic calcification and osteoporosis in Moscow Lung cancer screening: Is there a correlation between these findings?

Korkunova O.A. 1, Suchilova M.M. 1, Nikolaev A.E. 1, Grishkov S.M. 2, Gombolevskii V.A. 1, Bosin V.U. 1
1. Research and Practical Clinical Center of Diagnostics and Telemedicine Technologies, Department of Health Care of Moscow
2. Philips Russia and Central Asia

Aim

To assess the correlation between thoracic aortic calcification and osteoporosis in Moscow Lung cancer screening participants.

Materials and methods

A retrospective review included the results of 61 ultra-low-dose computed tomography (ultra-LDCT) performed in 57–87 year-old patients of whom 27 (44 %) were men and 34 (56 %) were women. The assessment of aortic calcification was performed only in this group. Agatston, Volume, and Mass indices for calcification of the ascending part, the arch, and the descending part of the thoracic aorta were quantitatively evaluated with semiautomatic method using OsiriX (picture 1). Quantitative evaluation of vertebral (Th 12, L1) bone mineral density (BMD) was performed with asynchronous QCT-densitometry.

Results

Quantitative evaluation of the aortic calcification severity was made with Agatston, Volume and Mass indices, as well as qualitative and quantitative analysis of the incidence of aortic calcification and osteoporosis in Lung cancer screening. The correlation between thoracic aortic calcification and BMD of vertebrae Th12-L1 was studied.

Conclusion

It is important to pay attention on the presence of thoracic aortic calcification when performing ultra-LDCT in lung cancer screening due to this change is associated with increased cardiovascular disease risk which may lead to death of the patient. Attention also must be paid to osteoporosis because its main complication is low-energy fractures development. Despite of the fact that there were no correlation between thoracic aortic calcification and osteoporosis in the study, the search for the correlation should be continued by measuring vertebral BMD at the level of aortic calcification where quantitative evaluation was performed which is an interesting task for further research.

Keywords:

aortic calcification, osteoporosis, ultra-low dose computed tomography

Korkunova Olga Andreevna
E-mail: oa.korkunova@gmail.com

Assessment of thoracic aortic calcification and osteoporosis in Moscow Lung cancer screening: Is there a correlation between these findings?

13

Introduction

Cardiovascular findings are often detected with a low-dose computed tomography (LDCT), which is used in lung cancer screening. For example, National Lung Cancer Screening Trial (NLST) reports that screening followed by treatment leads to 20 % reduction in lung cancer mortality and 6.7 % reduction in overall mortality [1]. Thus, LDCT was established as an informative technique for the examination of the chest organs, an important advantage of which is the use of low doses of irradiation compared with standard examination protocols. In 2017, "Moscow Lung cancer screening" project was launched in Moscow where LDCT was used for selective screening of lung malignancies in the outpatient care [2]. This project was powered by Research and Practical Clinical Center of Diagnostics and Telemedicine Technologies, Department of Health Care of Moscow.

Potentially dangerous conditions such as latent cardiovascular diseases in smokers are among the various types of pathology detected with ultra-LDCT screening [3]. In the NLST studies at least 50 % of deaths were associated with manifest or latent cardiovascular diseases as confirmed by observations in other cohorts, that necessitating the widespread use of screening methods [4]. One of the undoubted factors indicating the high risk of cardiovascular diseases is thoracic aortic calcification, which is associated with atherosclerosis, although the pathogenesis and clinical manifestations of this condition cause disputes among cardiologists at these time.

In 1994 the World Health Organization officially identified osteoporosis as an independent disease characterized by a decrease in the amount of bone mineral content that results in a partial loss of bone strength and increased risk of fractures. Osteoporosis is currently ranked fourth in the world after cardiovascular diseases, cancer, and sudden death according to the numerous multidisciplinary studies [5].

The main complications of osteoporosis are low-energy fractures developing due to a decrease in bone mass and deterioration of bone microarchitecture [6]. Bone mineral density (BMD) is used for quantitative evaluation of osteoporosis. BMD primarily characterizes the mechanical strength of the bone associated with calcium hydroxyapatite.

Osteopenia is a precursor to osteoporosis. Osteopenia is a condition characterized with low bone mass and the value for BMD 1.0–2.5 SD which is lower compared with BMD in young healthy population, but not has reached the osteoporosis level yet (T-score ranging from -1.0 to -2.5) [7]. These two pathological conditions can be assessed during lung cancer screening with ultra-LDCT if the CT scanner is calibrated and if there are lumbar spine scans. BMD can be measured quantitatively with quantitative computed tomography (QCT) provided that the study met these two criteria. QCT allows to estimate amounts of calcium (weight in grams) in the vertebral body [8].

Population studies shows that one in three women and one in four men over 50 years of age suffer from osteoporosis, but osteopenia is found in more than 40 % of both sexes in Russian Federation [7]. Since inclusion criteria in lung cancer screening with ultra-LDCT are asymptomatic people over 55 years of age with a smoking history (30 pack-year index > 30), we consider it relevant to assess BMD.

Table 1. *Diagnosis of osteoporosis based on the decrease of BMD according to WHO criteria for postmenopausal women and men over 50 years of age; osteoporosis assessment based on BMD (WHO)*

Classification	BMD	T-score
Normal rage	Within 1 standard deviation (SD) from the mean in the healthy young population	T-score ≥ -1.0
Osteopenia	Ranging from 1.0 to 2.5 SD lower than the mean in the healthy young population	T-score ranging from -1.0 to -2.5
Osteoporosis	Lower than 2.5 SD or more compared to the mean in the healthy young population	T-score ≤ -2.5
Severe osteoporosis	Lower than 2.5 SD or more compared to the mean in the healthy young population	T-score ≤ -2.5 in addition to 1 or more fractures

According to the literature, severe aortic calcification at the level of Th12 or abdominal region is the predictor of a decrease in bone mineral density as well as low-energy fractures development [9, 10, 11]. Recent data of both epidemiological and clinical studies showed that patients with low BMD are at significantly high risk of cardiovascular diseases (CVD) as well as unexpected cardiovascular events, more severe coronary atherosclerosis, and vascular calcification development [12-17].

Aim of the study

The aim of the study was to assess the prevalence of thoracic aortic calcification and osteoporosis in patients undergone lung cancer screening and to investigate the correlation between them.

Materials and methods

The retrospective study included ultra-LDCT scans, obtained from Toshiba Aquilion 64 (Canon Medical System, Japan) CT scanner, which was calibrated in order to perform quantitative evaluation of BMD based on QCT-densitometry data. All the examinations were performed according to ultra-LDCT protocols with tube voltage of 135 kV and different mAs depending on the patient's body weight (3 groups: < 69 kg, 70–89 kg, > 90 kg), tube rotation time around the table was 0.5 seconds and radiation load – 1 mSv, iterative reconstructions were not applied to achieve noise reduction.

The study included ultra-LDCT scans of the patients who met the following inclusion criteria for the lung cancer risk group: 55 years of age or older; patients with a smoking history with pack-years index > 30 and patients who gave up smoking less than 15 years ago; no history of lung, bronchus, and trachea cancer as well as no other cancer metastases in the lungs.

Agatston, Volume, and Mass indices for calcification of the ascending part, the arch, and the descending part of the thoracic aorta were quantitatively evaluated with semiautomatic method using OsiriX (picture 1). Quantitative evaluation of vertebral (Th 12, L1) bone mineral density (BMD) was performed with asynchronous QCT-densitometry.

Pearson and Spearman correlation coefficients were calculated in order to evaluate the correlation between thoracic aortic calcification and vertebral BMD at the level of Th12-L1 vertebrae.

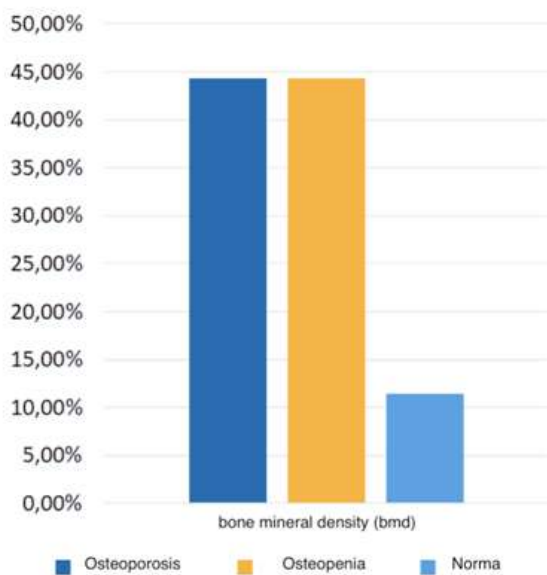*Picture 1. Semi-automatic segmentation of calcified thoracic aorta with OsiriX software*

Results

The study included the results of 61 ultra-LDCT performed in 57–87 year-old patients of whom 27 (44 %) were men and 34 (56 %) were women. These data were used only for the evaluation of aortic calcification and BMD.

Quantitative evaluation of the thoracic aortic calcification was made with Agatston, Volume and Mass indices and indicated that there were no calcinates in 10 % of cases, calcium score was less than 5000 in 55 % of cases, calcium score ranged from 5000 to 10000 in 25 % of cases, and calcium score was more than 10000 in 10 % of cases. It was also noted that the Agatston calcium score was higher in men than in women when detected by ultra-LDCT.

Quantitative evaluation of vertebral bone mineral density at the level of Th12-L1 vertebrae with QCT-densitometry showed that osteoporosis and osteopenia were detected with the same frequency (44.3 % of cases).

Assessment of thoracic aortic calcification and osteoporosis in Moscow Lung cancer screening: Is there a correlation between these findings?

15

Bone mineral density was within the normal range in 11.4 % of cases (Figure 1).



Figure 1. The incidence rates of osteopenia, osteoporosis and BMD within the normal range

Pearson correlation coefficient was 0 when estimating the correlation between thoracic aortic calcification and vertebral BMD, which shows no correlation between these two variables. Spearman's rank correlation coefficient was 0.14 that also reflects absence of any correlation.

Conclusion

Thoracic aortic calcification should be evaluated when performing lung cancer screening with ultra-LDCT as there changes are closely related to the high risk of cardiovascular diseases leading to death. It is also important to pay attention to osteoporosis because this condition is associated with low-dose fractures. Despite of the fact that this study did not reveal any correlation between two pathologies, the search should be continued by measuring vertebral BMD at the level of the part of aorta where the quantitative estimation was performed, which is an interesting task for further research.
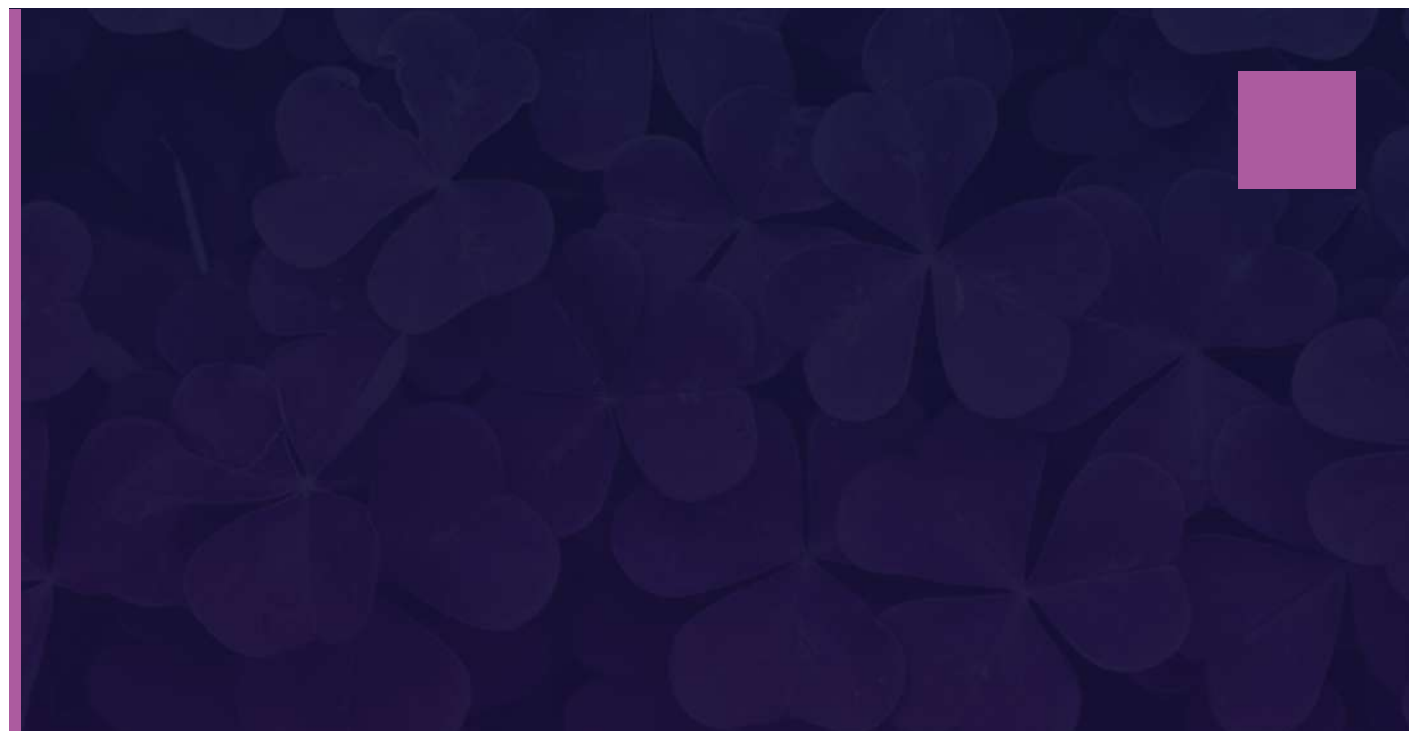
References:

1. National Lung Screening Trial Research Team, Aberle DR, Adams AM, et al: Reduced Lung-Cancer Mortality with LowDose Computed Tomographic Screening. N Engl J Med 365:395-409, 2011.

2. Гомболевский В.А., Харламов К.А.,Пятницкий И.А., Ким С.Ю., Морозов С.П. Шаблоны протоколов описаний исследований по специальности «рентгенология». Компьютерная томография. Методические рекомендации № 23 / Москва, 2016.

3. Incidental Findings on Lung Cancer Screening: Significance and Management Emily B. Tsai, MD, Caroline Chiles, MD, Brett W. Carter, MD, Myrna C.B. Godoy, MD, PhD, Girish S. Shroff, MD, Reginald F. Munden, MD, DMD, MBA, Mylene T. Truong, MD, and Carol C. Wu, MD.

4. Chiles C, Duan F, Gladish GW, et al. Association of coronary artery calcification and mortality in the national lung screening trial: a comparison of three scoring methods. Radiology. 2015 Jul; 276(1):82-90. doi:10.1148/radiol.15142062.

5. Низовцова Л.А., Морозов С.П., Петряйкин А.В., Босин В.Ю., Сергунова К.А., Владзимирский А.В., Шантаревич М.Ю. К УНИФИКАЦИИ ВЫПОЛНЕНИЯ И ИНТЕРПРЕТАЦИИ РЕЗУЛЬТАТОВ ОСТЕОДЕНСИТОМЕТРИИ. Вестник рентгенологии и радиологии. 2018;99(3):158-163. https://doi.org/10.20862/0042-4676-2018-99-3-158-163.

6. Мельниченко Г. А., Белая Ж. Е., Рожинская Л. Я. и др. Краткое изложение клинических рекомендаций по диагностике и лечению остеопороза Российской ассоциации эндокринологов // Остеопороз и Остеопатии. 2016. № 3. С. 28–36.

7. Годзенко А.В., Петряйкин А.В., Ким С.Ю., Морозов С.П., Сергунова К.А., Иванникова Н.В., Воронцов А.В., Киселёва Е.А. Остеоденситометрия / Серия «Лучшие практики лучевой и инструментальной диагностики».

8. Adams J. E. Quantitative computed tomography // Eur. J. Radiol. 2009. V. 71. № 3. P. 415–424.

9. Aortic Calcification and the Risk of Osteoporosis and Fractures. Eloy Schulz, Kiumars Arfai, Xiaodong Liu, James Sayre, Vicente Gilsanz. The Journal of Clinical Endocrinology & Metabolism, Volume 89, Issue 9, 1 September 2004, Pages 4246–4253. https://doi.org/10.1210/jc.2003-030964.

10. Zhou R, Zhou H, Cui M, Chen L, Xu J (2014) The Association between Aortic Calcification and Fracture Risk in Postmenopausal Women in China: The Prospective Chongqing Osteoporosis Study. PLoS ONE 9(5): e93882. https://doi.org/10.1371/journal.pone.0093882.

11. P. Szulc, D.P. Kiel, P.D. Delmas Calcifications in the abdominal aorta predict fractures in men: MINOS study J. Bone Miner. Res., 23 (2008), pp. 95-102. https://doi.org/10.1359/jbmr.070903.

12. Sinnott B, Syed I, Sevrukov A, Barengolts E. Coronary calcification and osteoporosis in men and postmenopausal women are independent processes associated with aging. Calcif Tissue Int. 2006;78(4): 195–202.

13. Von der Recke P, Hansen MA, Hassager C. The association between low bone mass at the menopause and cardiovascular mortality. Am J Med. 1999;106(3):273–278.

14. Esposito K, Capuano A, Sportiello L, Giustina A, Giugliano D. Should we abandon statins in the prevention of bone fractures? Endocrine. 2013;44(2):326–333.

15. Santos LL, Cavalcanti TB, Bandeira FA. Vascular effects of bisphosphonates-A systematic review. Clin Med Insights Endocrinol Diabetes. 2012;5:47–54.

16. Danilevicius CF, Lopes JB, Pereira RM. Bone metabolism and vascular calcification. Braz J Med Biol Res. 2007;40(4):435–442.

17. Kiel DP, Kauppila LI, Cupples LA, Hannan MT, O'Donnell CJ, Wilson PW. Bone loss and the progression of abdominal aortic calcification over a 25 year period: the Framingham Heart Study. Calcif Tissue Int. 2001;68(5):271–276

Assessment of thoracic aortic calcification and osteoporosis in Moscow Lung cancer screening: Is there a correlation between these findings?

17

Emphysema assessment with ultra-low dose computed tomography in Moscow Lung Cancer Screening.

Suchilova M.M.1, Korkunova O.A.1, Nikolaev A.E.2, Grishkov S.M. 2., Bosin V.Y.2.
1. FSBEI FPE RMACPE MON Russia
2. Research and Practical Clinical Center for Diagnostics and Telemedicine Technologies of the Moscow Health
Care Department, Moscow

Keywords:

emphysema, lung cancer, lung densitometry

Suchilova M.M.
E-MAIL: maria.suchilova@gmail.com

Introduction

Lung cancer is one of the most common oncological diseases and a leading cause of cancer death in the world [1]. According to the literature, lung cancer mortality in both sexes is the most frequent cause of cancer death through the years [2-6].

In Russia, such diseases as coronary heart disease (CHD), lung cancer and chronic obstructive pulmonary disease (COPD) are the most common causes of death. CHD has 1st, lung cancer - 6th and COPD - 10th places respectively in the distribution of disease and death according to WHO and the Institute for Health Metrics and Evaluation (IHME). Early detection and treatment of these conditions can influence the progression of the diseases and decrease the morbidity and mortality rates. In Russia, lung cancer has the first place in the cancer mortality rate among men [7-8]. Advanced lung cancer accounts for 70% of all the diagnosed cases of lung cancer in Russia and leads to death in 50% of cases within the 1st year. [10]. In 2017, the crude mortality rate for lung cancer was 34,18/100 000 (59,66 for males and 12,15 for females), the rate in Moscow was lower than in other Russian regions and reached 26,13/100 000 (40,46 for males and 13,82 for females) [9].

There were several attempts to use a low-dose computed tomography (LDCT) in lung cancer screening after computed tomography (CT) became commonly used. The major randomised trials are: DLST (Danish Lung Cancer Screening Trial) [11], MILD (Multicentric Italian Lung Detection) [12], ITALUNG [13], DANTE [14], LUSI [15], NLST (National Lung Screening Trial) [16].

LDCT allows to detect emphysema as well as focal lesions. A cohort study in lung cancer screening revealed that patients with COPD developed lung cancer 2-4 times frequently than patients without COPD [17, 18, 19, 20].

Emphysema as a predictor of COPD

Chronic obstructive pulmonary disease is a chronic life-threatening condition that gets worse over time. This disease is characterized by increasing breathlessness, poor airflow, exacerbations and may become severe [21]. The majority of patients with COPD are smokers.

Global epidemiological studies BOLD and PLATINO revealed that there are at least 600 million patients with COPD worldwide today [22, 23]. Global Initiative for Chronic Obstructive Lung Disease (GOLD) is the main document that standardized strategy for the management of COPD [24].

Spirometry is the standard test to detect COPD, the diagnosis considered to be certain when post-bronchodilator FEV1/FVC is < 0.7. COPD severity depends on symptoms and exacerbation frequency and it also must be remembered that early stages may be asymptomatic and, consequently, undetected. Recently, the US Preventive Services Task Force found that early detection of COPD in asymptomatic persons with spirometry does not improve health-related quality of life. There is no evidence of the efficacy of screening for COPD in asymptomatic adults using prescreening questionnaires and spirometry [25].

The method of early detection of COPD includes a quantitative assessment of emphysema, bronchial wall thickness and air trapping on chest CT scans. Quantitative assessment of emphysema is studied more than other signs of COPD mentioned above. Fully automatic quantitative assessment of emphysema in chest CT scans is more accurate than visual quantitative evaluation in chest CT scans or chest X-ray [26]. Regardless of the COPD stage, which was identified with pulmonary function tests, there is a strong correlation between the detection of emphysema on chest CT and lung cancer [27-30].

The "golden standard" of CT protocol and a threshold value for fully automatic quantitative assessment of emphysema are not developed yet. Emphysema could be quantitatively assessed with an automatic program for lung densitometry, which calculates the percentage of voxels based on the certain threshold value or lower it, usually from -910/-950 to -970 HU [31]. Moreover, the Perc15 technique, which identifies the HU meaning of the 15th percentile point of the lung density histogram [32]. The lower Perc15 value, i.e. closer to -1000 HU, the more severe emphysema is diagnosed. This method allows to classify single voxels as lung, emphysema or hyperinflation due to functional small airways disease.

Goals of the research

1. To evaluate the feasibility of emphysema diagnostics with ultra-low dose computed tomography (ULDCT) for lung cancer screening compared to routine CT.
2. To assess the prevalence of emphysema in ULDCT-based lung cancer screening in Moscow.

Materials and methods

ToshibaAquilion 64 and specially developed ULD CT scanning protocols with radiation-absorbed dose up to 1 mSv, which is used for chest X-ray screening in adults (SanRaN 2.6.1.1192-03), were used to perform examinations of patients with different weight.

Patients were included in the study according to the following enrolment criteria: 50 years of age or older; more than 30 pack-year smoking history; patients, who gave up smoking 15 years ago; no history of lung cancer, bronchial cancer or tracheal cancer; no history of lung metastases in patients with other cancers.

For preliminary evaluation of prevalence and severity of emphysema, a retrospective review of the results (images and reports) of ultra-low-dose chest computed tomography (ULD CT) that were performed in 2017 during project named "Moscow Screening for Lung Cancer" was done. The parameters were quantified for both ULD CT images and CT images, which were performed at 10 days interval.

The differences between CT indexes of emphysema, air trappings and bronchial wall thickness were evaluated on end-inhale and end-exhale ULD CT scans, which were performed as a part of the project "Moscow Screening for Lung Cancer" in 2017, with the use of Phillips Intellspace Portal 11.

Medical data was depersonalized according to personal data protection law. The analysis of DICOM 3.0 images was done with «AGFA Agility Enterprise 8.0» and «OsiriX MD (v.5.5.1 64-bit)» software. Philips Intellispace 4.0 was used for quantitive evaluation of emphysema.

Results

Smoking was one of the major inclusion criteria for it is known to be the cause of chronic obstructive pulmonary disease (COPD) in 79% of cases. 1678 participants (31,6%) of the lung cancer screening had a history of COPD. It is important to pay attention to such findings as emphysema and bronchial wall thickness, revealed during ULD CT screening for lung cancer, because it may help to detect early stages of COPD.

Regardless of the foci that could be classified with LungRads, incidental findings in the lungs were revealed in 68,5% (174/254) of cases. Primary LDCT reports included only 42,5% (74/174) of them.

The most frequent incidental findings on LDCT of the respiratory system included:
- thickening of the bronchial wall - 51,1% (90/174),
- emphysema - 31,65% (49/174),
- bronchiectasis - 51,1% (90/174),
- interstitial lung disease - 16,4% (29/174),
- thickening of parenchyma - 6,1% (11/174),
- pulmonary fibrosis - 22,3% (39/174).

Estimating weather emphysema was characterized in the reports the reports or not, we found that it was not mentioned in 24% of cases (12/49). Nearly half (51%, 30/49) of the radiologists did not characterized emphysema as centrilobular, panlobular, paraseptal, irregular.

Regardless of the difficulties in qualitative assessment of emphysema, ULD CT images could also be used to quantitative assessment. ULD CT and CT images (pic. 1) of the same patient, which were performed in 4 days interval end-inhale (the differences of volumes - 2,3%) are shown below. The patient has equal volumes of emphysema when threshold value for CT is -950HU and -933HU - for ULD CT.
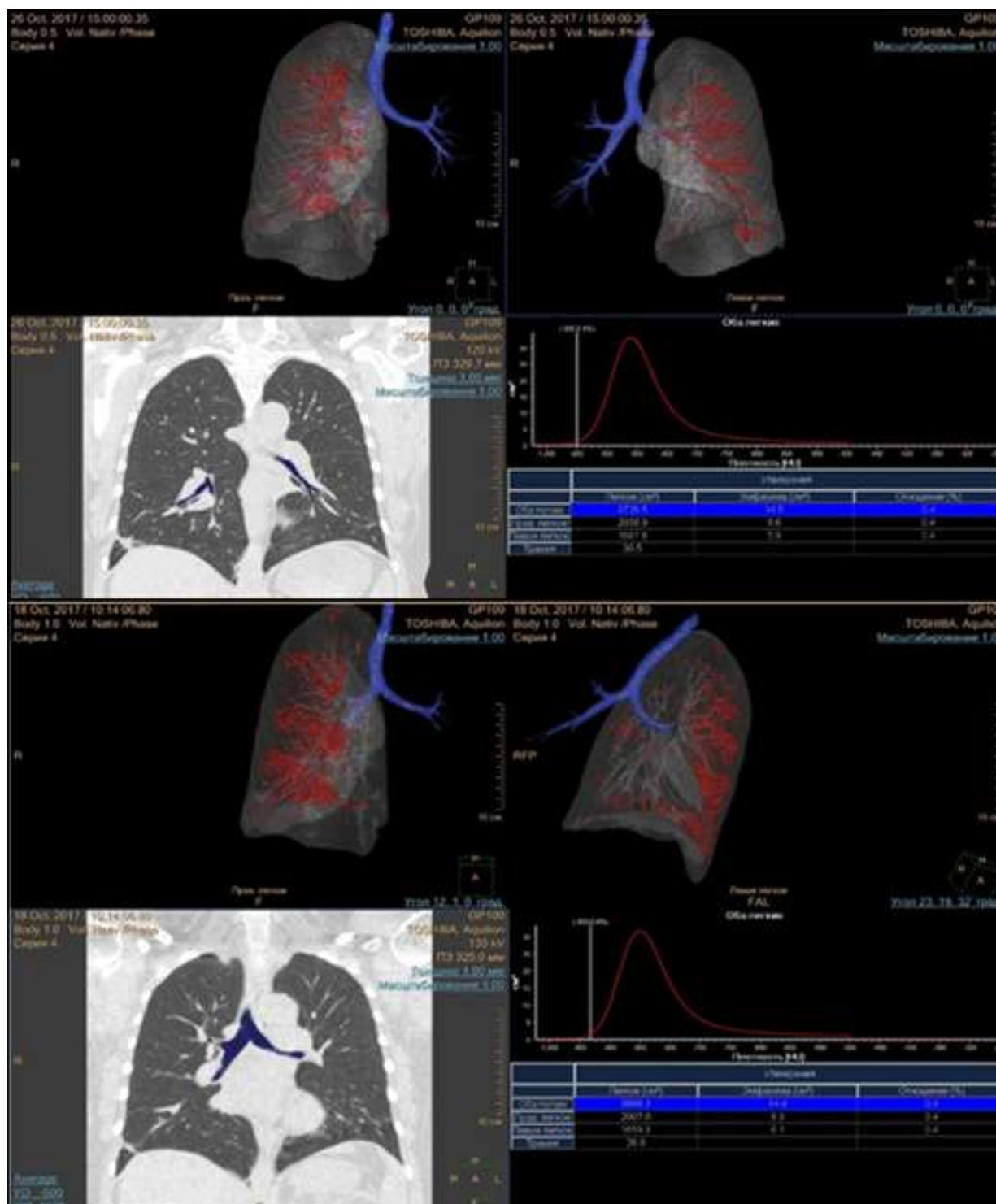
Picture 1. – Quantitative assessment of emphysema on CT and ULD CT images with different threshold values

---

Discussion

Pulmonary emphysema can be assessed not only qualitatively, but also quantitatively on and-inhale and end-exhale ULD CT data, which allows to evaluate the prevalence of the predictor of COPD in lung cancer screening in more details. Emphysema diagnosed with ULD CT in lung cancer screening should be studied in order to detect these diseases early. Screening for the predictor of COPD in addition to screening for lung cancer will significantly improve its efficacy and diagnostic significance.

References:

1. Bray F, Ferlay J, Soerjomataram I, Siegel RL, Torre LA, Jemal A. Global cancer statistics 2018: GLOBOCAN estimates of incidence and mortality worldwide for 36 cancers in 185 countries. CA Cancer J Clin. 2018 Nov;68(6):394-424. doi: 10.3322/caac.21492.

2. Aberle DR, Adams AM, Berg CD, Black WC, Clapp JD, Fagerstrom RM, Gareen IF, Gatsonis C, Marcus PM, Sicks JD. Reduced lung-cancer mortality with low-dose computed tomographic screening. N Engl J Med. 2011 Aug 4;365(5):395-409. doi: 10.1056/NEJMoa1102873

3. Bach PB, Mirkin JN, Oliver TK, Azzoli CG, Berry DA, Brawley OW, Byers T, Colditz GA, Gould MK, Jett JR, Sabichi AL, Smith-Bindman R, Wood DE, Qaseem A, Detterbeck FC. Benefits and harms of CT screening for lung cancer: a systematic review. JAMA. 2012 Jun 13;307(22):2418-29. doi:10.1001/jama.2012.5521

4. Field JK, Smith RA, Aberle DR, Oudkerk M, Baldwin DR, Yankelevitz D, Pedersen JH, Swanson SJ, Travis WD, Wisbuba II, Noguchi M, Mulshine JL. International association for the study of lung cancer computed tomography screening workshop 2011 report. J Thorac Oncol. 2012 Jan;7(1):10-19. doi: 10.1097/JTO.0b013e31823c58ab

5. Horeweg N, van der Aalst CM, Thunnissen E, Nackaerts K, Weenink C, Groen HJ, Lammers JW, Aerts JG, Scholten ET, van Rosmalen J, Mali W, Oudkerk M, de Koning HJ. Characteristics of lung cancers detected by computer tomography screening in the Randomized NELSON Trial. Am J Respir Crit Care Med. 2013 Apr 15;187(8):848-54. doi: 10.1164/rccm.201209-1651OC

6. Humphrey LL, Deffebach M, Pappas M, Baumann C, Artis K, Mitchell JP, Zakher B, Fu R, Slatore CG. Screening for lung cancer with lowdose computed tomography: a systematic review to update the US Preventive services task force recommendation. Ann Intern Med. 2013 Sep 17;159(6):411-20. doi: 10.7326/0003-4819-159-6-201309170-00690,

7. dop. Petrova GV, Kaprin AD, Grecova OP, Starinskij VV, red. Zlokachestvennye novoobrazovaniya v Rossii obzor statisticheskoj informacii za 1993-2013 gg. Moskva, RF; 2015. 259c.

8. dop. Kaprin AD, Starinskij VV, Petrova GV red. Zlokachestvennye novoobrazovaniya v Rossii v 2017 godu (zabolevaemost' i smertnost'). Moskva, RF; 2018. 9c.

9. dop. Kaprin AD, Starinskij VV, Petrova GV red. Zlokachestvennye novoobrazovaniya v Rossii v 2017 godu (zabolevaemost' i smertnost'). Moskva, RF; 2018. 180s.

10. Kaprin AD, Starinskij VV, Petrova GV red. Sostoyanie onkologicheskoj pomoshchi naseleniyu Rossii v 2017 godu. Moskva, RF; 2018. 96 s.

11. Wille MM, Dirksen A, Ashraf H, Saghir Z, Bach KS, Brodersen J, Clementsen PF, Hansen H, Larsen KR, Mortensen J, Rasmussen JF, Seersholm N, Skov BG, Thomsen LH, Tønnesen P, Pedersen JH. Results of the Randomized Danish lung cancer screening trial with focus on high-risk profiling. Am J Respir Crit Care Med. 2016 Mar 1;193(5):542-51. doi: 10.1164/rccm.201505-1040OC

12. Pastorino U, Rossi M, Rosato V, Marchianò A, Sverzellati N, Morosi C, Fabbri A, Galeone C, Negri E, Sozzi G, Pelosi G, La Vecchia C. Annual or biennial CT screening versus observation in heavy smokers: 5-year results of the MILD trial. Eur J Cancer Prev. 2012 May;21(3):308-15. doi: 10.1097/CEJ.0b013e328351e1b6

13. Paci E, Puliti D, Lopes Pegna A, Carrozzi L, Picozzi G, Falaschi F, Pistelli F, Aquilini F, Ocello C, Zappa M, Carozzi FM, Mascalchi M. Mortality, survival and incidence rates in the ITALUNG randomised lung cancer screening trial. Thorax. 2017 Sep;72(9):825-31. doi: 10.1136/thoraxjnl-2016-209825

14. Infante M, Lutman FR, Cavuto S, Brambilla G, Chiesa G, Passera E, Angeli E, Chiarenza M, Aranzulla G, Cariboni U, Alloisio M, Incarbone M, Testori A, Destro A, Cappuzzo F, Roncalli M, Santoro A, Ravasi G. Lung cancer screening with spiral CT: baseline results of the randomized DANTE trial. Lung Cancer.2008 Mar;59(3):355-63. doi: 10.1016/j.lungcan.2007.08.040

15. Becker N, Motsch E, Gross ML, Eigentopf A, Heussel CP, Dienemann H, SchnabelPA, Eichinger M, Optazaite DE, Puderbach M, Wielpütz M, Kauczor HU,

Tremper J, Delorme S. Randomized Study on Early Detection of Lung Cancer with MSCT in Germany: Results of the First 3 Years of Follow-up After Randomization. J Thorac Oncol. 2015 Jun;10(6):890-96. doi: 10.1097/JTO.0000000000000530

16. Lee YJ, Choi SM, Lee J, Lee CH, Lee SM, Yoo CG, Kim YW, Han SK, Park YS. Utility of the National Lung Screening Trial Criteria for Estimation of Lung Cancer in the Korean Population. Cancer Res Treat. 2018 Jul;50(3):950-55. doi: 10.4143/crt.2017.357

17. de Torres JP, Bastarrika G, Wisnivesky JP, et al. Assessing the relationship between lung cancer risk and emphysema detected on low-dose CT of the chest. Chest 2007;132:1932-8. 10.1378/chest.07-1490 [PubMed] [CrossRef] [Google Scholar]

18. Wilson DO, Weissfeld JL, Balkan A, et al. Association of radiographic emphysema and airflow obstruction with lung cancer. Am J Respir Crit Care Med 2008;178:738-44. 10.1164/rccm.200803-435OC [PMC free article] [PubMed] [CrossRef] [Google Scholar]

19. Maldonado F, Bartholmai BJ, Swensen SJ, et al. Are airflow obstruction and radiographic evidence of emphysema risk factors for lung cancer? A nested case-control study using quantitative emphysema analysis. Chest 2010;138:1295-302. 10.1378/chest.09-2567 [PubMed] [CrossRef] [Google Scholar]

20. Lowry KP, Gazelle GS, Gilmore ME, et al. Personalizing annual lung cancer screening for patients with chronic obstructive pulmonary disease: A decision analysis. Cancer 2015;121:1556-62. 10.1002/cncr.29225 [PMC free article] [PubMed] [CrossRef] [Google Scholar]

21. https://www.who.int/ru/news-room/fact-sheets/detail/chronic-obstructive-pulmonary-disease-(copd)

22. Buist A.S., Vollmer W.M., McBumie M.A. Worldwide burden of COPD in high- and low-income countries. Part I. The burden of obstructive lung disease (BOLD) initiative. Int. J. Tuberc. Lung. Dis. 2008; 12: 703—8.

23. Menezes A.M., Perez-Padilla R., Hallal P.C. et al. Worldwide burden of COPD in high- and low-income countries. Part II. Burden of chronic obstructive lung disease in Latin America: the PLATINO study. Int. J. Tuberc. Lung. Dis. 2008; 12: 709—12.

24. Global Strategy for the Diagnosis, Management, and Prevention of Chronic Obstructive Lung Disease: the GOLD science committee report 2019. Singh D, Agusti A, Anzueto A, Barnes PJ, Bourbeau J, Celli BR, Criner GJ, Frith P, Halpin DMG, Han M, López Varela MV, Martinez F, Montes de Oca M, Papi A, Pavord ID, Roche N, Sin DD, Stockley R, Vestbo J, Wedzicha JA, Vogelmeier C. Eur Respir J. 2019 May 18;53(5). pii: 1900164. doi: 10.1183/13993003.00164-2019. Print 2019 May. Review. PMID: 30846476

25. Siu AL, Bibbins-Domingo K, Grossman DC, et al. Screening for chronic obstructive pulmonary disease: US Preventive Services Task Force Recommendation Statement. JAMA. 2016;315:1372–1377.

26. Mets OM, Buckens CF, Zanen P, et al. Identification of chronic obstructive pulmonary disease in lung cancer screening computed tomographic scans. JAMA. 2011;306:1775–1781.

27. De Torres JP, Bastarrika G, Wisnivesky JP, et al. Assessing the relationship between lung cancer risk and emphysema detected on low-dose CT of the chest. Chest. 2007;132:1932–1938.

28. Wilson DO, Weissfeld JL, Balkan A, et al. Association of radiographic emphysema and airflow obstruction with lung cancer. Am J Respir Crit Care Med. 2008;178:738–744.

29. Zulueta JJ, Wisnivesky JP, Henschke CI, et al. Emphysema scores predict death from COPD and lung cancer. Chest. 2012;141:1216–1223.

30. Henschke CI, Yip R, Boffetta P, et al. CT screening for lung cancer: importance of emphysema for never smokers and smokers. Lung Cancer. 2015;88:42–47.

31. Labaki WW, Martinez CH, Martinez FJ, et al. The role of chest computed tomography in the evaluation and management of the patient with COPD. Am J Respir Crit Care Med. 2017;11:1372–1379.

32. Newell JD, Hogg JC, Snider GL. Report of a workshop: quantitative computed tomography scanning in longitudinal studies of emphysema. Eur Respir J. 2004;23:769–775.

CLINICAL CASES

Ischial bone apophysitis: a clinical case

Smorchkova A.K.1, Gonchar A.P.2, Blokhin I.A.2.

1. *I. M. Sechenov First Medical State University, Moscow, Russia.*
2. *Research and Practical Clinical Center of Diagnostics and Telemedicine Technologies, Department of Health Care of Moscow.*

Aim

To present a clinical case of ischial bone apophysitis.

Materials and methods

A 12-year old female patient with complaints on pubic pain and limited motion range.

Results

Computed tomography initially detected an avulsion fracture. To further evaluate the ischial bone, magnetic resonance imaging was done, revealing a left-sided apophysitis.

Conclusion

Multimodal imaging in the form of CT an MRI is pivotal for diagnostics of apophyses lesions. The radiologist must account for the normal age-related musculoskeletal findings. Such awareness allows for correct and timely diagnosis affecting patient management and treatment outcomes.

Keywords:

ischial bone apophysitis, computed tomography, magnetic resonance imaging.

Gonchar Anna Pavlovna
E-MAIL: anne.gonchar@gmail.com

Relevance

Ischial apophysitis (apophyseal osteochondropathy, subacute inflammatory process) is a common trauma among children aged 13–15 years, occurring during the period of active growth (Fig. 1) [1].
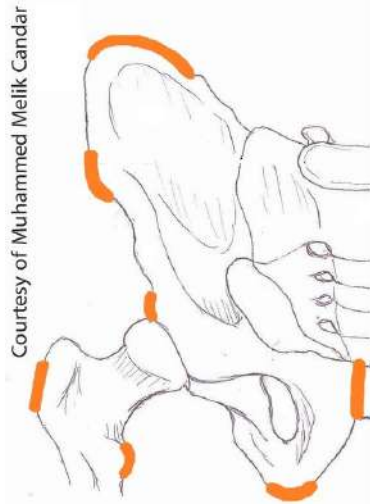
*Figure 1. Schematic representation of bony pelvis with apophyses highlighted in orange*

Before their synostosis, apophyses are prone to detachment or inflammation [2]. The pathological conditions are most common among physically active children involved in gymnastics, basketball, football. Ischial avulsion injury is caused by "pullup" jump or falls from a great height. Apophysitis develops gradually with regular stress on the biceps femoris, semimembranosus, and semitendinosus muscles. After synostosis, the same injuries usually lead to stretching of muscles mentioned above [1].

Clinically, apophysitis manifests as discomfort and exercise-related pain, especially with stretching. Prolonged rest alleviates the pain. Inadequate rest or treatment combined with continuous exercise will exacerbate the patient's condition, impeding an active lifestyle.

Normal apophysis on radiographs and computed tomography is often interpreted as avulsion fractures that may occur during physical exertion.

Clinical case

A 12-year old female was admitted to the Department of Pediatric Traumatology with complaints of persistent pain in the pubic area and difficulty in performing the left longitudinal splits. She was professionally engaged in artistic gymnastics. Per the complaints above, the patient was hospitalized in the Department of Pediatric Traumatology with subsequent pelvic CT scan. The report indicated an ischial avulsion fracture (Fig. 2). We performed magnetic resonance imaging to assess the ligaments and muscles of the posterior compartment of the thigh. The scan did not reveal any ligamentous injury nor ischial avulsion fracture. T2 and STIR images detected edema of the ischial bone (anterior and posterior branches) (Fig. 3 a, b, c).
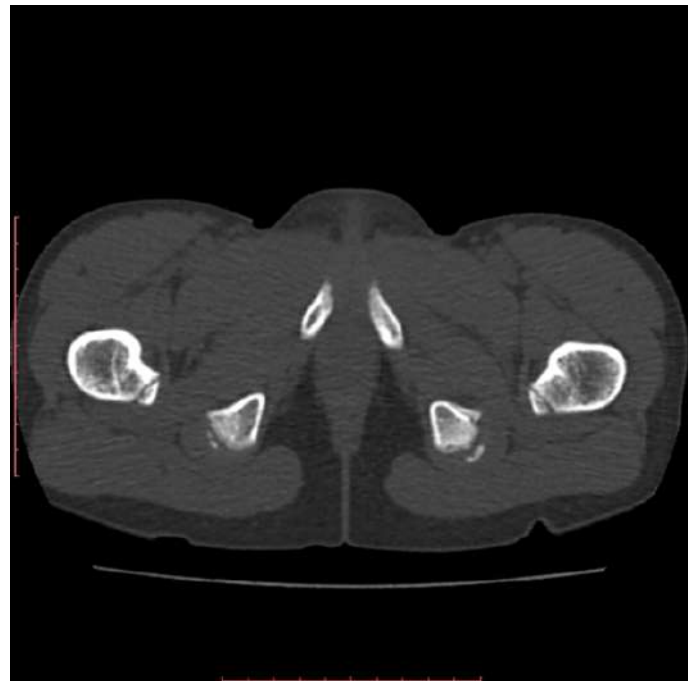
Figure 2. Pelvic CT scan. Axial slice, bony window. Well-defined bony lesions with distinct margins are present in the area of the ischial tuberosities. The ischial bones have fuzzy contours posteriorly. The depicted lesions are apophyses with developing ossification centers.

Discussion

The apophysis is the normal bony outgrowth arising from an ossification center and subsequently fusing with the bone. Ligaments and muscles of the posterior thigh compartment attach to the ischial apophysis. The ischial ossification center develops between the ages of 13–15 years and exists until the full synostosis at 16–25 years. In the pediatric population, the ligaments and tendons are stronger than the attachment site; therefore, excessive loads cause damage to the apophysis. After synostosis intense physical activity can lead to muscle strain or rupture. Repetitive sports-related traction loads on posterior thigh compartment muscles can cause apophysitis.

Apophysitis diagnostics requires an integrated approach. Careful history taking, physical examination, and radiography improve diagnostic accuracy and allow prescribing adequate treatment. Usually, it includes the avoidance of physical activities and the prescription of anti-inflammatory medication [1].

Apophysitis has to be differentiated with an ischial avulsion fracture and musculoligamentous injury. As such, the probability of misdiagnosis with X-ray or CT is rather high. For example, an impression of apophysiolysis can lead to surgical intervention. Therefore, the preferred radiological method in apophysitis is MRI, allowing for accurate lesion detection and treatment response evaluation.

In the acute phase of ischial apophysitis, MRI shows increased signal on T2-weighted images and decreased signal on T1-weighted images, corresponding to edema. This clinical case is an illustration of these changes. Edema resolves with treatment and rest, possibly leaving sclerotic changes, depicted as low signal on all pulse sequences [3].

The prevention of acute and chronic traumatic injuries is essential, especially for young athletes. Sports physicians and trainers need to educate the athletes on the features of immature musculoskeletal system and risks of apophysitis or avulsion fracture [1]. Many athletes seldom have this information, increasing the trauma likelihood, delays appropriate therapy, and adequate rehabilitation. All this can lead to a vicious cycle with complications, decreased quality of life due to chronic pain, and abrupt termination of a sports career [1].

The prevention of the trauma mentioned above includes limiting intensive training during the growth spurt [1]. Therefore, measurements are taken every three months. The training regimen should exclude repetitive strenuous exercises, which can lead to trauma. In this scenario, quality is more important than quantity. The regular monitoring of an athlete's physical health has to be a vital part of the program. During the recovery period in apophysitis, it is necessary to exclude contact sports for up to 6 months. At the same time, radiological follow-up is carried out at intervals of 3-6 months for two years [4, 5].

Conclusion

Thus, when a young athlete visits a doctor with complaints of pain associated with intense regular physical exertion, the doctor must act quickly. A multimodal radiological investigation (CT and MRI) will help to perform differential diagnostics in the shortest possible time correctly. In turn, timely treatment initiation and a lengthy rehabilitation period are the keys to returning to sports without any short or long-term risks.

Figure 3. Pelvic MRI scan. Coronal slices. T2 (a) and STIR (b) images reveal the hyperintense signal in the left ischial bone. In T1 (c) images, the region of interest has a hypointense signal. This corresponds to edema of the left ischial bone. Т костей таза. Коронарная проекция. На Т2 (а) и Т2 STIR (б).

References

1. Umile Giuseppe Longo, Mauro Ciuffreda, Joel Locher, Nicola Maffulli, Vincenzo Denaro. Apophyseal injuries in children's and youth sports. British Medical Bulletin. Volume 120, Issue 1, 1 December 2016, Pages 139–159, https://doi.org/10.1093/bmb/ldw041

2. Calderazzi F, Nosenzo A, Galavotti C, Menozzi M, Pogliacomi F, Ceccarelli F. Apophyseal avulsion fractures of the pelvis. A review. ABM . 15 Nov. 2018; 89(4):470-6

3. Kujala, U., Orava, S., Karpakka, J., Leppävuori, J., & Mattila, K. (1997). Ischial Tuberosity Apophysitis and Avulsion Among Athletes. International Journal of Sports Medicine, 18(02), 149–155. doi:10.1055/s-2007-972611

4. Koehler SM, Rosario-Quinones F, Mayer J, et al. Understanding acute apophyseal spinous process avulsion injuries. Orthopedics 2014;37:e317–21.

5. Launay F. Sports-related overuse injuries in children. Orthop Traumatol Surg Res 2015;101:S139–47.

PRACTICAL PART

Mastitis visualization and BI-RADS

Suchilova M.M.1, Korkunova O.A.1, Tarachkova E.V. 1, Nikolaev A.E.2, Khadartseva M.P. 3, Gombolevskii V.A.2

1. *FSBEI FPE RMACPE MOH, Russia*
2. *Research and Practical Clinical Center of Diagnostics and Telemedicine Technologies, Department of Health Care of Moscow, Russia*
3. *European Medical Center, Moscow*

Mastitis

Mastitis is an inflammation of the breast tissue that most frequently occurs in breastfeeding women.

Symptoms:

- Breast swelling
- Pain
- Breast skin redness
- Fever, general soreness
- Nipple retraction
- Lymphadenopathy

Epidemiology [1]:

- Regardless of breastfeeding prevalence, mastitis can be observed in different social groups.
- The official incidence of mastitis may be low or reach 33% of breastfeeding women, but commonly the rate is 10% or less.
- Mastitis most commonly occurs during the second or third weeks after delivery.
- However, this condition may be observed in every week of lactation period and even 2 years after the delivery.

Etiology:

- Plugged duct
- Infection
  » frequent - Staphylococcus aureus and Staphylococcus AlbusStaphylococcus aureus и Staphylococcus Albus
  » rare - Escherichia coli, Streptococcus (α-, β- and nonhemolytic), M. Tuberculosis

Predisposing factors:

- Age (from 21 to 35 y.o.)
- First labor
- Previous cases of mastitis
- Food (salt and fat overconsumption, lack of microelements)
- Delivery complications
- Lack of immune factors in breast milk
- Stress
- Trauma
- Full-time job

Classifications:

Clinical forms:
- Serous
- Infiltrative
- Abscessed
- Phlegmonous
- Gangrenous
- Chronic infiltrative

Localization:
- Superficial premammary and subarealar
- Intramammary
- Retromammary
- Diffuse mastitis

Title	Causes	Verification	Risk group
Acute mastitis	lactational (90%) and non-lactational	ill-defined lesions with increased density; skin thickening;	Young women with recent delivery or lactation
Plasma cell mastitis [2]	A rare form, not associated with infections	rod-like or cigar-shaped calcifications	Women over 60 years of age
Granulomatous mastitis [4], [6]	A very rare disease associated mostly with tuberculosis, sarcoidosis, mycosis, may be idiopathic (diagnosis based on exclusion)	Verified with histologic features	Young women with recent delivery or lactation
Lymphocytic mastitis (lymphocytic mastopathy/ sclerosing lymphocytic lobulitis/ Diabetic mastopathy) [8-9]	A rare autoimmune condition that can mimic breast cancer and may affect both mammary glands	Core biopsy	Women with autoimmune conditions and diabetes mellitus

Biopsy:

- Ultrasound-guided fine needle biopsy is used for differential diagnosis of inflammatory and malignant diseases.
- Core biopsy, vacuum biopsy, and excisional biopsy are used for establishing the diagnosis with a histologic pattern.

Imaging methods:

- Mammography
- US
- Tomosynthesis
- MRI

In the first instance, young women should undergo US examination in order to eliminate an abscess. Antibiotic treatment is used for confirming the diagnosis. Trial treatment should always be performed before MRI, which is to be used for differential diagnosis between inflammatory breast cancer and mastitis. Biopsy should not be delayed in cases when clinical findings are suspicious for cancer [5]. Women over 40 should undergo mammography.

Ultrasound findings:

- skin thickening;
- diffusely increased echo in subcutaneous fat;
- decrease of the distinction between derma and the subcutaneous fat;
- decrease of the distinction of each structure of the breast parenchyma;
- single or multiple hypoechoic lesions in breast parenchyma, well or poorly defined;
- dilated milk ducts, presence of one or several cystic cavities of milk ducts;
- enlarged axillary lymph nodes.

Ultrasound findings strongly correlate with the intensity of clinical symptoms [3].
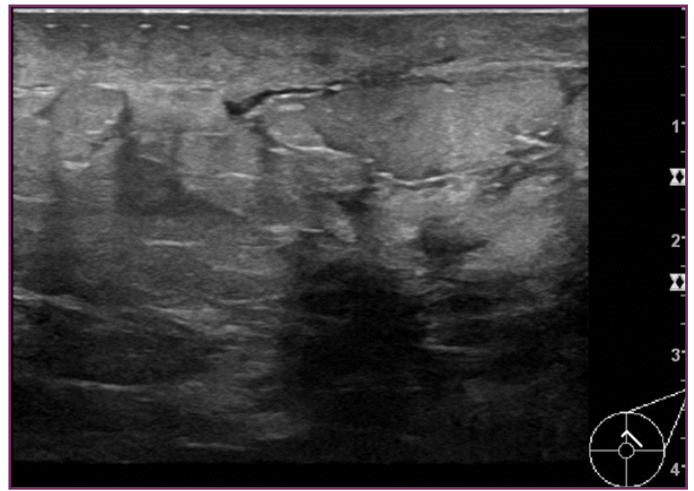
Picture 1. Nonsuppurative non-lactational mastitis
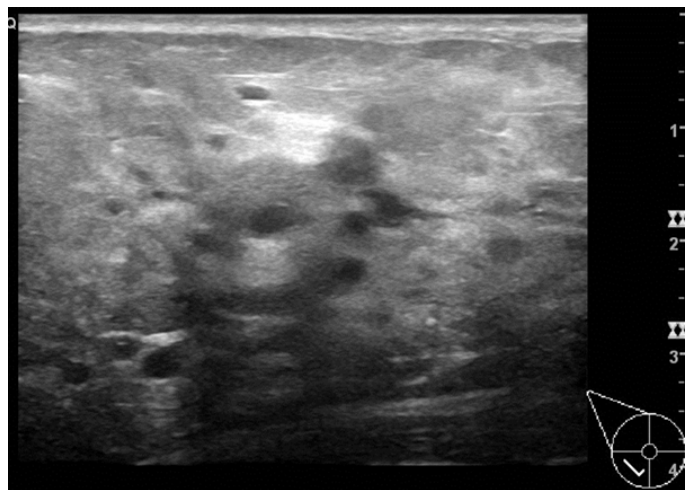
Picture 2. Nonsuppurative lactational mastitis
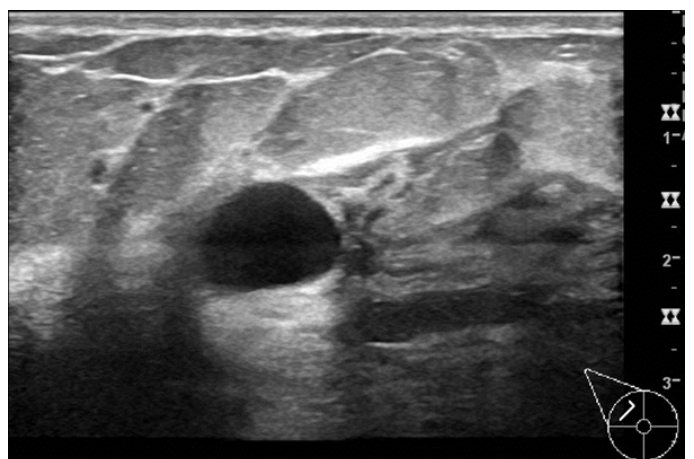
Picture 3. Abscess (suppurative non-lactational mastitis), Staphylococcus epidermidis.

Mammography findings:

- Ill-defined high-density lesions;
- Skin thickening.

Mammography report should include:

- Indications for investigation (screening, diagnostic);
- Type of the breast tissue structure;
- Evaluation of the skin, nipples, ducts, lymph nodes;
- Nodular lesions, calcifications, changes of the lymph nodes;
- Comparison with the previous mammograms;
- BI-RADS category;
- Recommendations about additional examinations, specialist medical consultations, the time of the follow up mammography.

MRI findings [11]

T1-WI
Low signal intensity (55%)
Iso-signal intensity (45%)
T2-WI
Homogeneous high signal (27%)
Heterogeneous high signal (73%)
T1+C (Gd)
Non-mass-like (90%)
Mass-like (10%)
Skin thickening (33%)

BI-RADS was developed by American College of Radiology and allows to standardize mammography, ultrasound and MRI reports.

| BI-RADS categories	Recommendations	Risk of malignancy
BI-RADS 0 – incomplete	Additional imaging evaluation	Non-applicable
BI-RADS 1 – no changes	Routine screening	0%
BI-RADS 2 – benign findings	Routine screening	0%
BI-RADS 3 – probably benign findings	Short-interval follow-up (6 months)	0-2%
BI-RADS 4 – suspicious abnormality	Biopsy	
BI-RADS 4A	Low suspicious of malignancy	2-10%
BI-RADS 4B	Moderate suspicious of malignancy	10-50%
BI-RADS 4C	High suspicious of malignancy	50-95%
BI-RADS 5 – highly suggestive of malignancy	Biopsy	Выше 95%
BI-RADS 6 – known biopsy-proven malignancy	Surgical excision when clinically appropriate	Non-applicable

Management of breast MRI-detected lesions is determined with the algorithm below: [7]
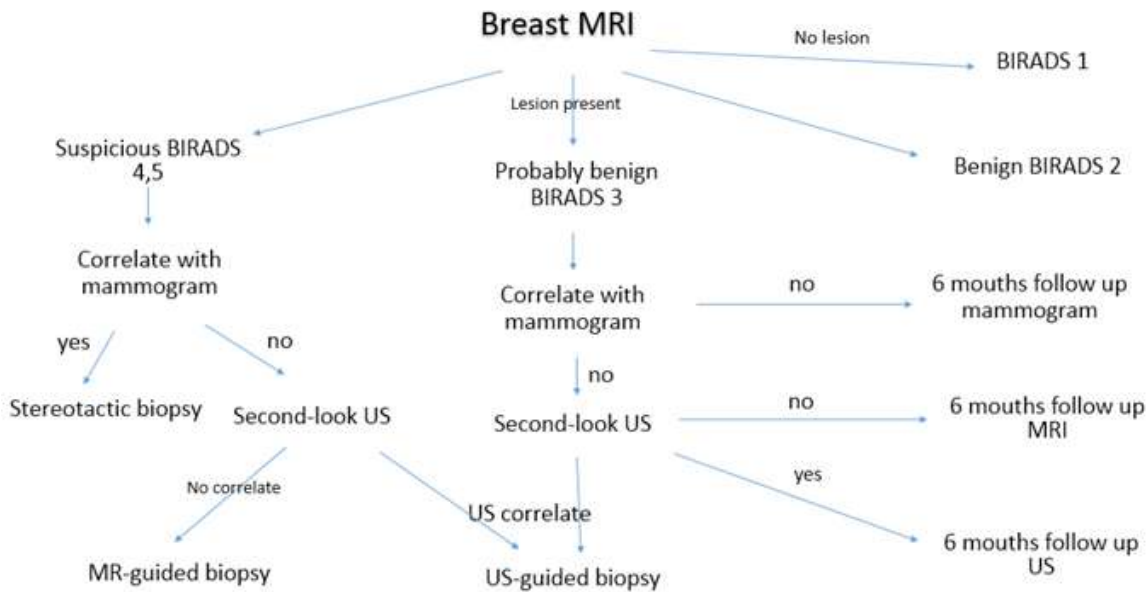
The generally accepted scheme for indicating the localization of lesions in the mammary gland:
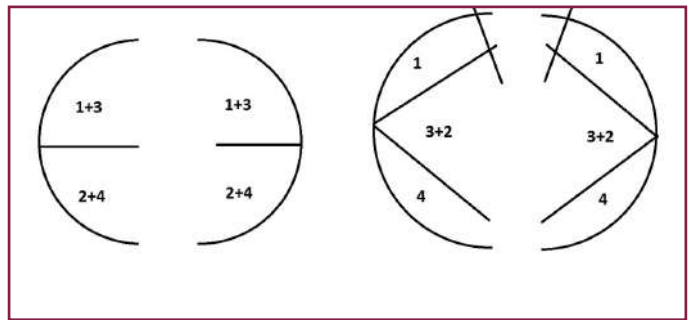
1 - upper outer quadrant
2 - upper inner quadrant
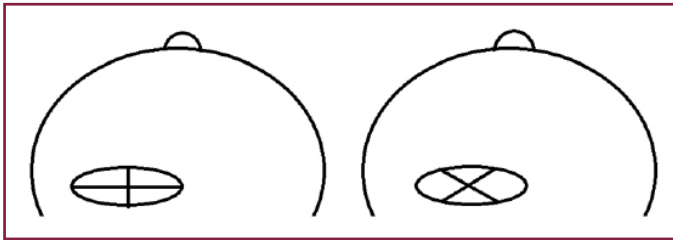3 - lower outer quadrant
4 - lower inner quadrant
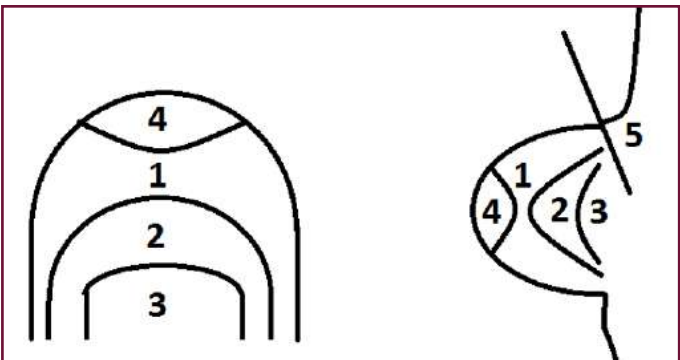
1 - anterior
2 - middle (corpus mammae)
3 - posterior (Chassaignac's bursa)
4 - subareolar
5 - axillary tail
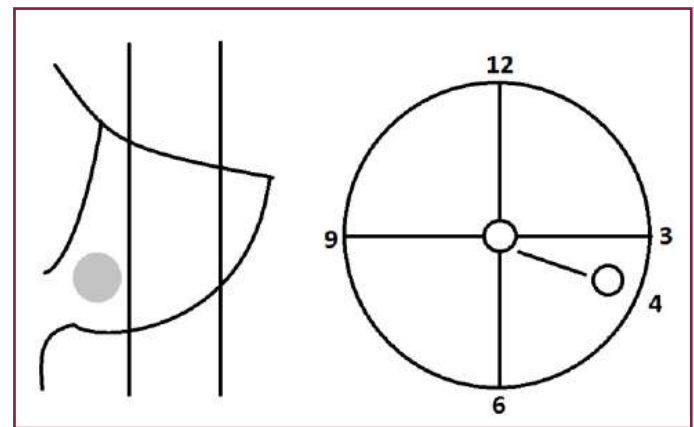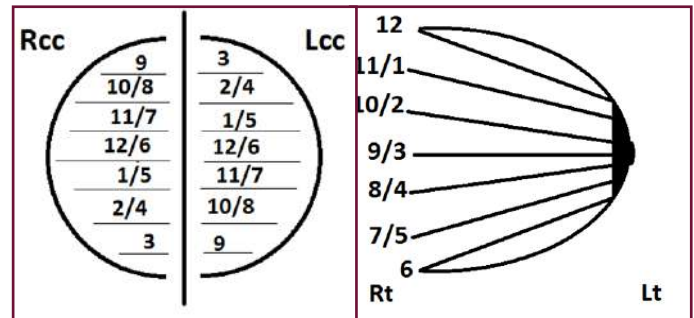
Localization:
- Quadrant and o'clock position
- Depth
- Distance from the nipple to the lesion

NB! In order to measure the lesion correctly one should use the rule – perpendicular to the maximum length!

Complications

An abscess is the result of the acute mastitis. Ultrasound findings of a typical abscess: a single cavitary lesion with thick hypoechoic capsule and anechoic heterogenous content, which is the result of tissue necrosis [3].

The abscess may be classified according to clinical signs, localization and causative microorganisms (Staphylococcus aureus, Staphylococcus epidermidis, Streptococcus pyogenes, and anaerobes such as Peptostreptococcus and Bacteroides. There are also lactational and non-lactational abscesses.

Differential diagnosis

Inflammatory breast cancer
• A rare and very aggressive type of breast cancer, accounts for only 1-5% of all cases of breast cancer.
• Women at the age of 40-50.

References:

1. Мастит. Причины и ведение / Всемирная органи-зация здравоохранения. - Женева: ВОЗ, 2000. - 46 с.

2. Sickles EA. Breast calcifications: mammographic evaluation. Radiology. 1986;160 (2): 289-93

3. Yilmaz E, Lebe B, Usal C et-al. Mammographic and sonographic findings in the diagnosis of idiopathic granulomatous mastitis. Eur Radiol. 2001;11 (11): 2236-40. doi:10.1007/s003300100965

4. Cedric W. Pluguez-Turull , Jennifer E. Nanyes, Cristina J. Quintero, Hamza Alizai, Daniel D. Mais, Kenneth A. Kist, Nella C. Dornbluth Idiopathic Granulomatous Mastitis: Manifestations at Multimodality Imaging and Pitfalls

5. Sharifah Majedah Idrus Alhabshi,1,2 Kartini Rahmat,2 Caroline Judy Westerhout,2 Nani Harlina Md Latar,3Patricia Ann Chandran,4 and Suraya Aziz1 1 Lymphocytic Mastitis Mimicking Breast Carcinoma, Radiology and Pathology Correlation: Review of Two Cases Malays J Med Sci. 2013 May; 20(3): 83–87. PMCID: PMC3743988 PMID: 2396683

6. Sabaté JM, Clotet M, Gómez A et-al. Radiologic evaluation of uncommon inflammatory and reactive breast disorders. Radiographics. 2005;25 (2): 411-24. doi:10.1148/rg.252045077

7. D. Groheux , M. Chapellier , F. Sabatier , A. Scémama , A. Pluvinage , M. Albiter , E. de Kerviler Breast inflammation: Indications for MRI and PET-CT C. de Bazelaire*

8. Сенча А. Н., Ультразвуковая мультипараметриче-ская диагностика патологии молочных желез М. : ГЭОТАР-Медиа, 2017. - 360 с. - ISBN 978-5-9704-4229-6 -

9. Tan H, Li R, Peng W, Liu H, Gu Y, Shen X. Br J Radiol. Radiological and clinical features of adult non-puerperal mastitis. 2013 Apr;86(1024):20120657. doi: 10.1259/bjr.20120657. Epub 2013 Feb 7. PMID: 23392197

10. Jean M.SeelyMDCM Management of Breast Magnetic Resonance Imaging-Detected Lesions, FRCPC

11. Isabelle Trop , Alexandre Dugas, Julie David, Mona El Khoury, Jean-François Boileau, Nicole Larouche, Lucie Lalonde Breast Abscesses: Evidence-based Algorithms for Diagnosis, Management, and Follow-up

A systematic approach to a cystic pattern in the lungs

Mukhutdinova G. Z.1, Tkacheva P. V.1, Nikolaev A. E.2, Blokhin I. A.2, Chernina V.Yu.2, Gombolevskyi V. A.2, Grishkov S.M.3

1. Pirogov Russian National Research Medical University Ostrovitianov
2. Research and Practical Clinical Center of Diagnostics and Telemedicine Technologies, Department of Health Care of Moscow
3. Philips-healthcare in Russia and Central Asia.

Keywords:

Nikolaev Alexander
E-MAIL: a.e.nikolaev@yandex.ru

Cystic lung disease is a broad term used to describe pathological process in the lungs, characterized by the presence of cysts in the lung parenchyma.

A cyst is any round circumscribed space that is surrounded by an epithelial or fibrous wall of variable thickness.

Radiographs and CT scans

A cyst appears as a round parenchymal lucency or low-attenuating area with a well-defined interface with normal lung [1].

Cysts have variable wall thickness but are usually thin-walled (<2 mm) and occur without associated pulmonary emphysema. Cysts in the lung usually contain air but occasionally contain fluid or solid material.

The term is often used to describe enlarged thin-walled airspaces in patients with lymphangioleiomyomatosis or Langerhans cell histiocytosis; thickerwalled honeycomb cysts are seen in patients with end-stage fibrosis [1].

A cavity is a gas-filled space, seen as a lucency or low-attenuation area, within pulmonary consolidation, a mass, or a nodule. In the case of cavitating consolidation, the original consolidation may resolve and leave only a thin wall. A cavity is usually produced by the expulsion or drainage of a necrotic part of the lesion via the bronchial tree. It sometimes contains a fluid level. Cavity is not a synonym for abscess [1].

A pseudocavity appears as an oval or round area of low attenuation in lung nodules, masses, or areas of consolidation that represent spared parenchyma, normal or ectatic bronchi, or focal emphysema rather than cavitation. These pseudocavities usually measure less than 1 cm in diameter. They have been described in patients with adenocarcinoma, bronchioloalveolar carcinoma, and benign conditions such as infectious pneumonia [1].

Figure 1. *In this image are presented a cyst (left), a cavity (center), a pseudo-cavity (right)*

A pneumatocele is a thin-walled, gas-filled space in the lung. It is most frequently caused by acute pneumonia, trauma, or aspiration of hydrocarbon fluid and is usually transient.

The mechanism is believed to be a combination of parenchymal necrosis and check-valve airway obstruction. A pneumatocele appears as an approximately round, thin-walled airspace in the lung [1].

A bleb is a small gas-containing space within the visceral pleura or in the subpleural lung, not larger than 1 cm in diameter.

A bleb appears as a thin-walled cystic air space contiguous with the pleura. Because the arbitrary (size) distinction between a bleb and bulla is of little clinical importance, the use of this term by radiologists is discouraged [1].

Bulla is an airspace measuring more than 1 cm—usually several centimeters—in diameter, sharply demarcated by a thin wall that is no greater than 1 mm in thickness. A bulla is usually accompanied by emphysematous changes in the adjacent lung.

A bulla appears as a rounded focal lucency or area of decreased attenuation, 1 cm or more in diameter, bounded by a thin wall. Multiple bullae are often present and are associated with other signs of pulmonary emphysema (centrilobular and paraseptal) [1].
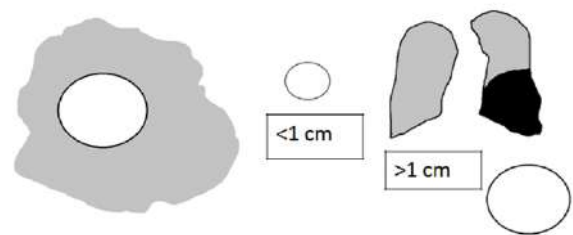
Figure 2. *In this image are presented a pneumatocele (left), bleb (center), bull (right)*

An air crescent is a collection of air in a crescentic shape that separates the wall of a cavity from an inner mass.

The air crescent sign is often considered characteristic of either Aspergillus colonization of preexisting cavities or retraction of infarcted lung in angioinvasive aspergillosis. However, the air crescent sign has also been reported in other conditions, including tuberculosis, Wegener granulomatosis, intracavitary hemorrhage, and lung cancer [1].

Cystic bronchiectasis is irreversible localized or diffuse bronchial dilatation, usually resulting from chronic infection, proximal airway obstruction, or congenital bronchial abnormality.

Morphological criteria for CT scans include bronchial dilation relative to the accompanying pulmonary artery, lack of bronchial constriction, and visualization of the bronchi within 1 cm of the pleura surface [1].

Honeycombing represents destroyed and fibrotic lung tissue containing numerous cystic airspaces with thick fibrous walls, representing the late stage of various lung diseases, with complete loss of acinar architecture.

The cysts range in size from a few millimeters to several centimeters in diameter, have variable wall thickness, and are lined by metaplastic bronchiolar epithelium. On chest radiographs, honeycombing appears as closely approximated ring shadows, typically

3–10 mm in diameter with walls 1–3 mm in thickness, that resemble a honeycomb; the finding implies end-stage lung disease. On CT scans, the appearance is of clustered cystic air spaces, typically of comparable diameters on the order of 3–10 mm but occasionally as large as 2.5 cm.

Honeycombing is usually subpleural and is characterized by well-defined walls. It is a CT feature of established pulmonary fibrosis. Because honeycombing is often considered specific for pulmonary fibrosis and is an important criterion in the diagnosis of usual interstitial pneumonia, the term should be used with care, as it may directly impact patient care [1].
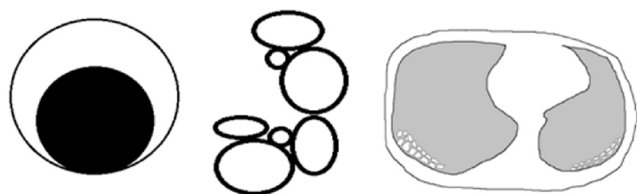
Figure 3. *In this image are presented a air crescent sign (left), cystic bronchiectasis (center), honeycomb lung (right)*

The authors of Maffessanti and Dalpiaz distinguish certain types of cystic changes or patterns characterized by multiple areas of low density with smooth contours in relation to normal pulmonary parenchyma.

For example, such as:
- Cystic changes in the type of grape cluster.
- Cystic changes in the type of pearl thread.

Cystic changes in the type of grape cluster - close to each other brush along the bronchi vascular pedicle, usually localized in the upper and middle zones. This type of changes is typical for cystic bronchiectasis, cystic fibrosis [1].

Distribution:	Uni- or Bilateral
Axial plane:	Central or the peripheral zones
Craniocaudal plane:	Upper and middle zones
Certain diagnosis:	Cystic bronchiectasis Cystic fibrosis

Cystic changes along the string of pearls are characterized by the location of one row of cysts in the subpleural zones, usually in the upper and middle zones, which is characteristic of paraseptal emphysema [1].

Distribution:	Uni- or Bilateral
Axial plane:	Peripheral and subpleural areas
Craniocaudal plane:	Upper and middle zones
Certain diagnosis:	Paraseptal emphysema

Honeycomb lung, detected by CT, is a specific change in pulmonary fibrosis and is an important criterion in the diagnosis of usual interstitial pneumonia (UIP), so the term should be used with caution, as it can directly affect the tactics of patient management. Depending on additional symptoms such as traction bronchiectasis, reticular changes, pleural plaques, subpleural changes, either the UIP pattern, asbestos, collagenosis is suspected [1].

Distribution:	Bilateral
Axial plane:	Peripheral and subpleural zones
Craniocaudal plane:	Basal, peripheral zones
Differential diagnosis:	UIP, Asbestosis, Collagenosis

A cystic pattern with a random cyst distribution is visualized as cysts arranged arbitrarily. For the differential diagnosis it is also necessary to evaluate the distribution in the craniocaudal direction with the assessment of the costal-diaphragmatic angles [2].

The tables below show two different types of cystic pattern with random cysts:

Distribution:	Bilateral, symmetrical
Axial plane:	Uniform distribution
Craniocaudal plane:	Upper, middle zones
Differential diagnosis:	Centrilobular emphysema, Langerhans cell histiocytosis

Distribution:	Bilateral, symmetrical
Axial plane:	Uniform distribution
Craniocaudal plane:	Diffuse
Certain diagnosis:	**Lymphangioleiomyomatosis**

Further in the review are not considered:
- Single air cysts – e.g. pneumatocele
- Fluid-filled cysts – e.g. echinococcal cyst
- Honeycomb lung / end-stage fibrosis
- Cystic bronchiectasis

Cysts, as a dominant sign on CT, are characteristic of many diseases [2]:
1. Langerhans cell histiocytosis
2. Lymphangioleiomyomatosis
3. Lymphoid interstitial pneumonia
4. Centrilobular emphysema
5. Tracheobronchial papillomatosis
6. gren
7. Follicular bronchiolitis
8. Cystic fibrosis
9. Asbestos-induced pneumoconiosis
10. Neurofibromatosis
11. Syndrome Berta-Hogan-Dube (rarely)
12. Pulmonary mesenchymal cystic hamartoma (rarely)
13. Light chain disease
14. Subacute hypersensitive pneumonitis

Cysts, as an additional sign, occur in the following pathologies [2]:
1. Cystic bronchiectasia
2. Desquamative interstitial pneumonia
3. Cell light in the pattern of the IPR
4. Lung injury
5. Pneumocystis pneumonia
6. Sarcoidosis
7. Pulmonary metastases (squamous/adenocarcinoma)
8. Cystic fibrohistiocytoma lung tumor
9. Cystic mesenchymal
10. Necrobiotic nodules (final stage)

When assessing cystic changes in the lungs, the following signs should be taken into account:
- Distribution (craniocaudal, axial plane)
- Number
- Uni-, bilateral changes.
- Additional typical changes typical of other nosologies
- Changes in surrounding parenchyma
- Form of cystic changes

Particular attention should be paid to clinical manifestations, as sometimes the assumption of a diagnosis is out of the question, if there is no clinical data, even better when there is pathomorphological verification.

Lymphangioleiomyomatosis.
Lymphangioleiomyomatosis is a tumor growth of smooth muscle fibers in the interstitial.
Options: local form (leiomyoma) and diffuse form (cysts)
Clinical symptoms: first of all – it is shortness of breath.
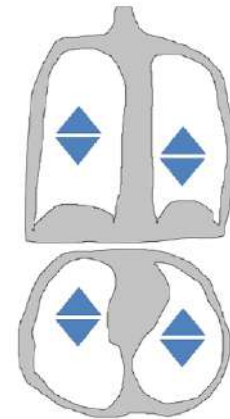
More often affects women of childbearing age, receiving estrogen therapy, the connection of shortness of breath with menstruation, pregnancy, combination with uterine myoma.

Additional symptoms - spontaneous pneumothorax (50-80%), chylous pleurisy (– 20-40%), pericarditis, ascites.

The function of external respiration (spirometry) – norm or obstructive changes.

Radiography – mesh deformation, sometimes visible air cysts, pleurisy, pneumothorax.

According to CT data, cysts are usually visualized without clearly visible walls against the background of an unchanged pulmonary parenchyma. However, nodes are not typically rendered.

Additional signs include pneumothorax, lymphadenopathy, pleural effusion and others, such as renal angiolipoma.

Uniform distribution of cysts, less pronounced in the tops of the lungs.

Bronchovascular trunk is stored in the walls of cysts (may resemble bronchiectasis) [2].

Distribution:	Bilateral, symmetrical
Axial plane:	Uniform distribution
Craniocaudal plane:	Diffuse
Differential diagnosis:	Lymphangioleiomyomatosis

Langerhans cell histiocytosis

Langerhans cell histiocytosis is a term for a group of diseases with unexplained etiology, in which pathological immune cells, called histiocytes, and eosinophils actively multiply, especially in the lungs and bones, which causes the formation of scar tissue.

Morphology – proliferation in organs and tissues of Langerhans cells

– Consolidation around bronchioles and arterioles include lymphocytes, neutrophils and eosinophils

- Symptoms: fatigue, weight loss, fever, dry cough
- Additional symptoms: smokers (70-95%), predominantly male (4:1), spontaneous pneumothorax (15-25%)
- Respiratory Function – a combination of obstruction and restriction
- Radiography – nodes/reticulation in the upper lobes – tuberculosis

CT-picture depends on the stage of the process

- Initial stage – centrilobular nodes in upper and middle

lung sections – respiratory bronchiolitis (open biopsy)

- At a late stage – lung cysts – irregular shape, outlined

the walls are combined with micro foci (typical pattern) as presented in the middle images

The lower images show additional features of centrilobular nodules less than 10 mm in diameter with cavitations, to the right of the pneumothorax proper [2].
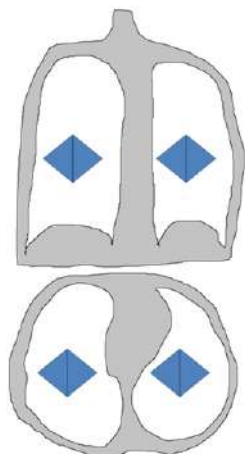
Distribution:	Double-sided, symmetrical
Axial plane:	Uniform distribution
Craniocaudal plane:	Upper, middle
Differential diagnosis:	Lymphangioleiomyomatosis, Centrilobular emphysema, Cystic bronchiectasis

Lymphoid interstitial pneumonia, or LIP

LIP is a rare disease characterized by diffuse pulmonary lymphoid proliferation with predominant interstitial involvement. It is included in the spectrum of interstitial pneumonias and is distinct from diffuse lymphomas of the lung.

Features include diffuse hyperplasia of bronchus-associated lymphoid tissue and diffuse polyclonal lymphoid cell infiltrates surrounding the airways and expanding the lung interstitium. LIP is usually associated with autoimmune diseases or human immuno-deficiency virus infection.

Ground-glass opacity is the dominant abnormality, and thin- walled perivascular cysts may be present. Lung nodules, a reticular pattern, interlobular septal and bronchovascular thickening, and wide-spread consolidation may also occur.

Clinical manifestations – shortness of breath, dry cough (50%), fatigue (80%), fever (40%), arthralgia (30%), weight loss (30%)

Physical signs – crepitation (70%), drumsticks (10%)

FVD – restrictive type, reduced diffusion capacity

Radiography – possible reticular changes in the basal regions.

According to CT data, single pulmonary cysts, which can be combined with a symptom of frosted glass (reversible) or be the only manifestation of the disease.
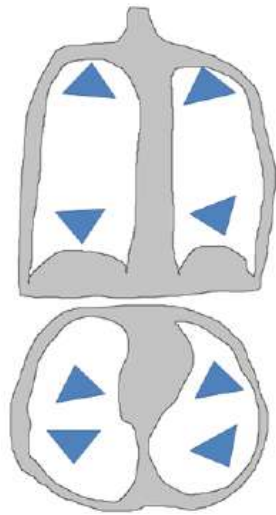
Emphysema

Emphysema is a permanent and irreversible pathological expansion (usually destruction) of air-containing spaces distal to terminal bronchioles without concomitant fibrosis.
Classification
- Proximal acinar emphysema
  – Centrilobular and focal
- Distal acinar (paraseptal) emphysema
- Panacinar emphysema

Changes in x-ray is manifested by the local depletion of lung pattern and avascular areas, architectural distortion For panacinar emphysema is characterized by diffuse expansion of acinus, the merger of intra-lobular structures into a single airspace with predominant localization in the lower lobes of the lungs.

Additional signs are thickening of the bronchial wall, signs of pulmonary hypertension, intraluminal changes in the trachea, lymphadenomegaly, which are caused by chronic inflammation [1].
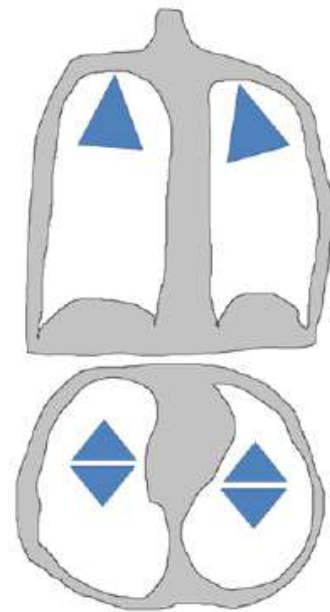
Asbestos-induced pneumoconiosis

Asbestos is a form of pneumoconiosis that develops as a result of long-term inhalation of asbestos-containing dust and is characterized by diffuse fibrosis of the pulmonary tissue. This pathology is also characterized by visualization of cysts from 2 to 10 mm, which are usually located in the posterior subpleural areas forming a cellular lung. Usually, in this pathology, the lungs are reduced in volume, the changes are bilateral against the background of bronchial and bronchiolectasis [1].

From other indications I would also like to acknowledge the presence:
- reticular changes,
- subpleural lines and bands,
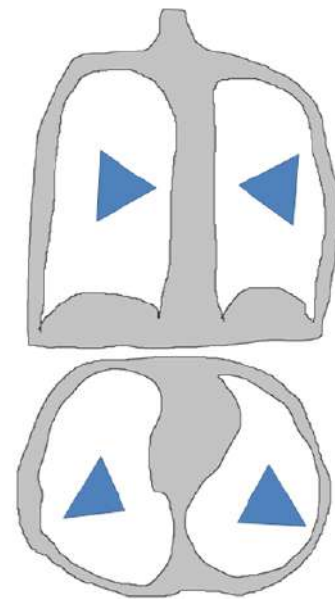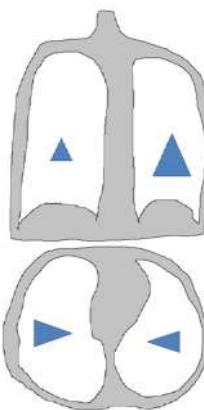- pleural plaques,
- thickening of the pleura.

Cystic fibrosis

Cystic fibrosis is a systemic hereditary disease caused by a mutation of the gene of the transmembrane regulator of cystic fibrosis and characterized by damage to the glands of external secretion, severe violations of the functions of the respiratory organs.

According to CT data in the axial plane changes are usually centrally arranged in pairs, but it is also worth paying attention to the peripheral zones. Cranio-caudal distribution predominance in the upper lobes and dorsal segment of the lower lobes, especially on the right.

Additional changes in the form of changes in the type of mosaic density and cylindrical bronchiectases filled with air [3].

Distribution:	Bilateral
Axial plane:	Central perihilar but also periphery
Craniocaudal plane:	Predominance in the upper lobes and dorsal segment of the lower lobes, especially in the right lung
Differential diagnosis:	Allergic bronchopulmonary aspergillosis Langerhans Histiocytosis Tracheobronchomalacia

Tracheobronchial papillomatosis

Tracheobronchial papillomatosis is characterized by the appearance of multiple squamous papillomas in the trachea and bronchi. This is an unusual manifestation of recurrent respiratory papillomatosis (RRP), which in itself is a rare phenomenon in which HPV-associated papilloma is localized along the respiratory, digestive tract.

Usually CT shows thin-walled cysts with adjacent nodes of 2-3 mm in size. With a more common disease, normalization can be observed. On CT it is also possible to visualize the distal atelectasis, bronchiectasis and bronchi clogged with mucus [4].


Sjogren's syndrome (scleroderma)

This pathology is characterized by visualization of cysts from 2 to 10 mm, which are usually located in the posterior subpleural areas, forming a honeycomb lung. Usually the lungs are reduced in volume, bilateral changes in the background of traction bronchi- and bronchiolectasis.

Among other signs: intralobular reticular changes, subpleural lines and strands, unilateral thickening of the pleura, esophageal dilation [5].
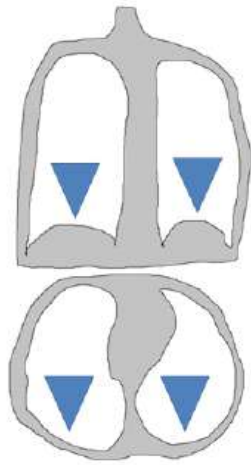
Distribution:	Bilateral
Axial plane:	Peripheral, predominantly subpleural posterior
Craniocaudal plane:	Basal parts
Differential diagnosis:	Asbestosis Collagenosises UIP

Light chain deposition disease (BOLC)

Light chain deposition disease (BOLC) is a rare systemic disease based on the deposition of monoclonal light chains in various organs and tissues, which leads to a progressive impairment of their function.
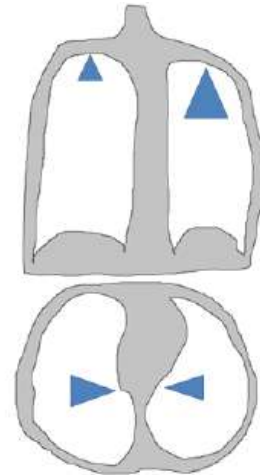
In the manifestation of the disease, the deposition of light chains on CT visualized cysts, lymphadenopathy, nodules. It is believed that the formation of the cyst comes from the wall of the small respiratory tract [6].
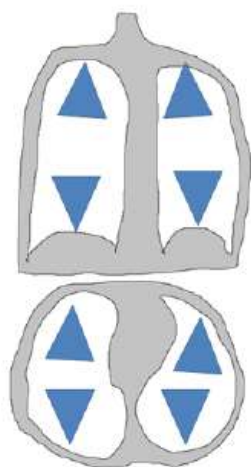
Cystic bronchiectasis

Cystic bronchiectasis is irreversible localized or diffuse bronchial dilatation, usually resulting from chronic infection, proximal airway obstruction, or congenital bronchial abnormality.

Morphological criteria for CT scans include bronchial dilation relative to the accompanying pulmonary artery, lack of bronchial constriction, and visualization of the bronchi within 1 cm of the pleura surface [1].


Distribution:	Bilateral
Axial plane:	Peripheral, predominantly subpleural posterior
Craniocaudal plane:	Basal parts
Differential diagnosis:	Cavitating metastases Histiocytosis Of Langerhans Plasma cell pneumonia

Desquamative interstitial pneumonia, or DIP

Histologically, DIP is characterized by the widespread accumulation of an excess of macrophages in the distal airspaces. The macrophages are uniformly distributed, unlike in respiratory bronchiolitis–interstitial lung disease, in which the disease is conspicuously bronchiolocentric. Interstitial involvement is minimal. Most cases of DIP are related to cigarette smoking, but a few are idiopathic or associated with rare inborn errors of metabolism.

Ground-glass opacity is the dominant abnormality and tends to have a basal and peripheral distribution. Microcystic or honeycomb changes in the area of

ground-glass opacity are seen in some cases [1].
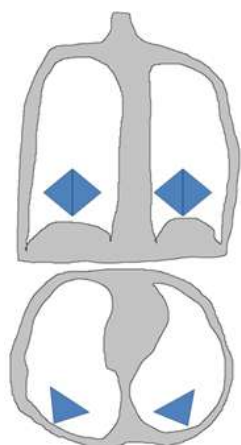
Usual interstitial pneumonia, or UIP

Usual interstitial pneumonia in the later stages is also visualized with the presence of cysts, the manifestations of which are naturally not in the first place.

UIP is a histologic pattern of pulmonary fibrosis characterized by temporal and spatial heterogeneity, with established fibrosis and honeycombing interspersed among normal lung. Fibroblastic foci with fibrotic destruction of lung architecture, often with honeycombing, are the key findings. The fibrosis is initially concentrated in the lung periphery. UIP is the pattern seen in idiopathic pulmonary fibrosis, but can be encountered in diseases of known cause [1].

| Distribution:	Bilateral
Axial plane:	Peripheral, predominantly subpleural posterior
Craniocaudal plane:	Basal part
Differential diagnosis:	Collagenosises Asbestosis Sarcoidosis
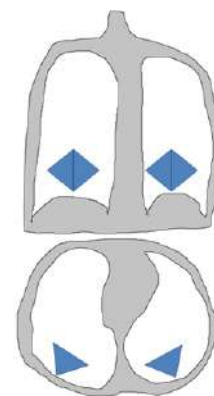
Cystic lung cancer and metastases

Cystic metastases also have a differential diagnosis in patients with a history of cancer, which should be differentiated from cavitating metastases [7]. During the first year, 4,700 ultra-LDCT were performed in the risk group, and of 84 verified malignancies in the lungs, almost 5% had signs of pseudo-cavities according to ultra-LDCT.
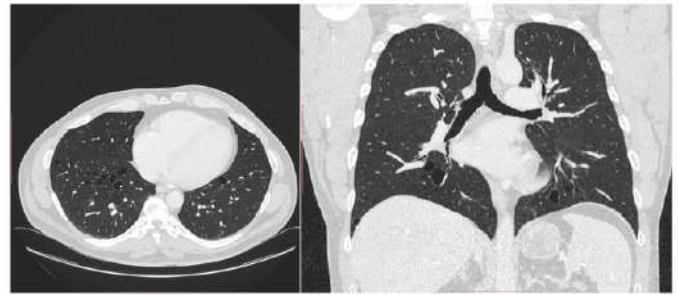
Birt–Hogg–Dubé syndrome

Birt–Hogg–Dubé syndrome is a rare autosomal dominant genetic disease caused by mutation in the FLCN gene and manifested by the development of benign tumors of the hair follicle, cysts in the lungs and an increased risk of kidney cancer and colon cancer.

On CT images, signs of manifestation of the syndrome are usually manifested by bullous emphysema, thin-walled cysts, pneumothorax [8].
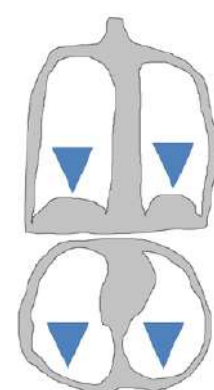
Below is a CT image of this rare disease. Note the distribution of cystic changes in the lower lung and subpleural localization, as well as the absence of pneumothorax. The disease is verified by genetic tests.

Figure 4. *CT scan of a patient with Birt–Hogg–Dubé syndrome.*

References:

1. Fleischner Society: Glossary of Terms for Thoracic Imaging David M. Hansell, Alexander A. Bankier, Heber MacMahon, Theresa C. McLoud, Nestor L. Müller, Jacques Remy Mar 1 2008 - https://doi.org/10.1148/radiol.2462070712

2. Diffuse Lung Diseases Clinical Features, Pathology, HRCT Editors: Maffessanti, Mario, Dalpiaz, Giorgia (Eds.), 2006

3. AG SK, Karger. Cystic Fibrosis, A State-Of-The-Art Series. S Karger Pub. (2001) ISBN:3805572247.

4. Ko JM, Jung JI, Park SH et-al. Benign tumors of the tracheobronchial tree: CT-pathologic correlation. AJR Am J Roentgenol. 2006;186 (5): 1304-13. doi:10.2214/AJR.04.1893

5. Ito I, Nagai S, Kitaichi M et-al. Pulmonary manifestations of primary Sjogren's syndrome: a clinical, radiologic, and pathologic study. Am. J. Respir. Crit. Care Med. 2005;171 (6): 632-8. doi:10.1164/rccm.200403-417OC

6. Colombat M, Stern M, Groussard O et-al. Pulmonary cystic disorder related to light chain deposition disease. Am. J. Respir. Crit. Care Med. 2006;173 (7): 777-80. doi:10.1164/rccm.200510-1620CR

7. Simion NI, Pezzetta E. Cystic appearance: an uncommon feature of pulmonary metastasis of colorectal origin. BMJ Case Rep. 2011;2011 (dec12 1): . BMJ Case Rep (full text) - doi:10.1136/bcr.10.2011.5063 - Pubmed citation

8. Steinhoff M, Kinzel M, Krahl D. White papules on the face, neck and upper chest. Birt-Hogg-Dubé syndrome. J Dtsch Dermatol Ges. 2012;10 (9): 665-7. doi:10.1111/j.1610-0387.2012.07971.x

ANATOMY

Mammary gland: anatomy

Krysanova Aleksandra Vladimirovna
resident in the department of radiology in «N.N. Blokhin National Medical Research Center of Oncology» of the Ministry of Health of the Russian Federation
Address: *Kashirskoe sh. 23, Moscow, Russia*
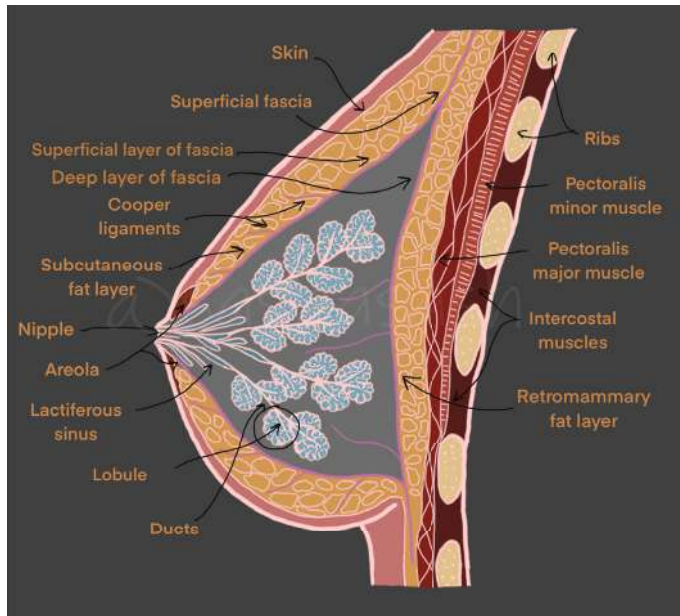***E.mail:*** *doctor.krysanova@gmail.com,*
ORCID: *0000-0002-7640-5296*
SPIN: *3661-9078*

The mammary gland (MG) is a compound tubuloalveolar organ. MG is derived from a sweat gland and made up of 15–20 lobes. Extent: from the II rib to the VII rib.

Medial border of the gland - lateral border of the sternum.

Lateral border of the gland - anterior axillary line. [1] (picture 1)

There are three main components of the gland:
1. Connective tissue
2. Adipose tissue
3. Glandular tissue

MG is surrounded by superficial and deep layers of the superficial fascia of the anterior thoracic wall. These layers form the mammary gland capsule.

The superficial fascia is attached to the clavicle and forms suspensory ligament of the mammary gland.

The superficial and deep layers are linked by the connective tissue – Cooper's ligaments [1].

Adipose component include premammary fat, retromammary fat as well as adipose tissue located between the gland lobes.

Glandular tissue forms the mammary lobes (picture 2). Their amount correlates with the gland size. The MG lobe is comparable to a small branch of grape consisting of lobules (grapes). Lobe and lobule do not have capsule and considered to be functional units of the mammary gland. [2]

The distribution of glandular tissue in the MG is irregular. Most of the tissue is located within the upper outer quadrant where the pathological changes are most commonly found.
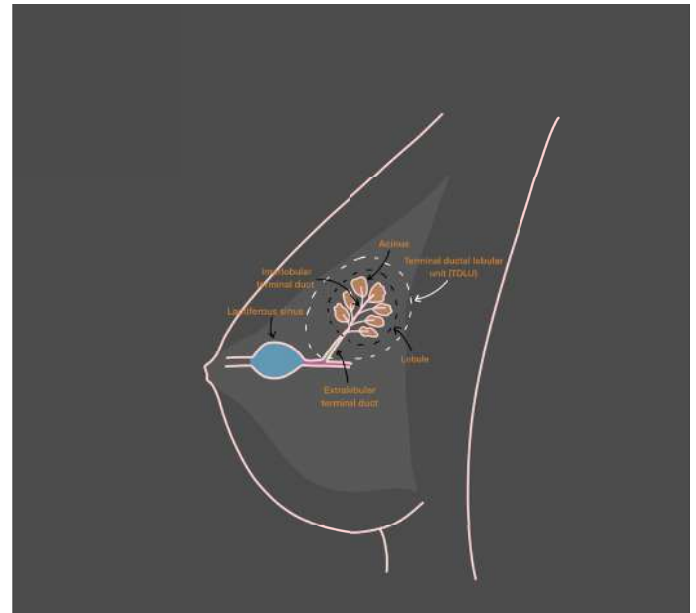
The ductal system of MG consists of galactophores and lactiferous sinuses. Every lobule has size 1 galactophore, when confluencing they form size 2 and 3 galactophores. Size 3 galactophore has a dilation near the nipple - lactiferous sinus.

MG duct sizes:
- Size 3 galactophore ≤ 3 mm
- Size 2 galactophore ≤ 2 mm
- Size 1 galactophore ≤ 1 mm

Mammary gland anatomy is not constant and depends on age and endocrine profile. Proliferation of lobular and ductal epithelium begins after menarche and becomes active a few days before ovulation every month. The newly formed structures undergo atrophy if pregnancy does not occur. Proliferation slows and MG tissue involution begins in postmenopausal period [2].

Radiological anatomy of the mammary gland

There is no common radiological standard for the mammary gland due to the fact that every woman has a different ratio of fibroglandular and adipose components.
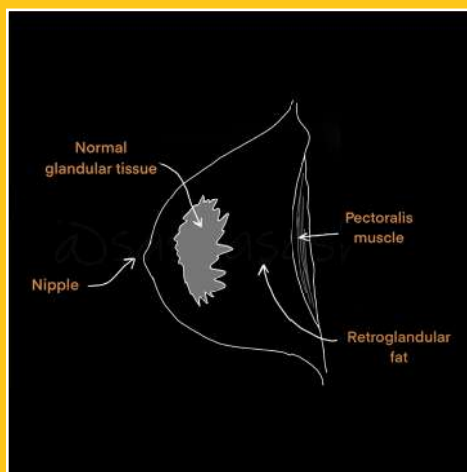
There are several types of gland density according to this ratio.

The mammograms clearly show skin, premammary fat, areola, nipple, Cooper's ligaments, glandular tissue, and retromammary space. [2] (pictures 3–6)
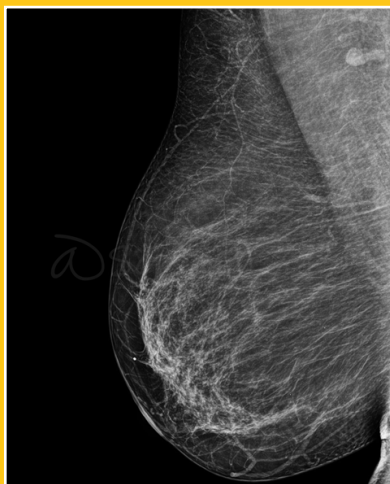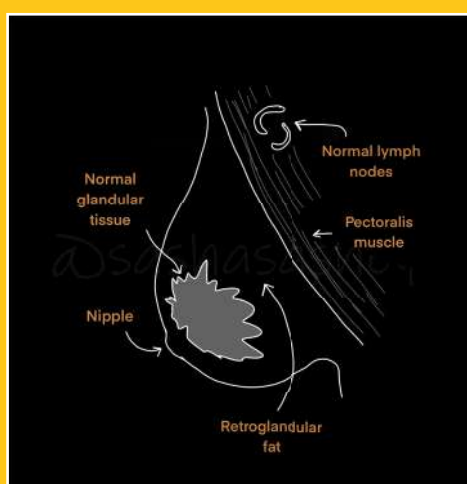
Picture 3
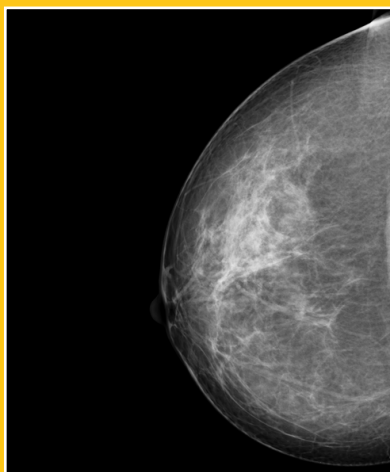
Picture 4

Picture 5

Picture 6

The skin on mammograms looks like a straight line 1–2 mm thick. Subcutaneous fat is straight behind the skin. Normally, it looks more transparent than the skin and glandular tissue. [4]

Glandular tissue looks like a cone the base of which is attached to pectoral fascia and the top ends with a nipple. Structural elements of glandular tissue cannot be differentified on non-contrast enhanced mammograms. [3]

The retromammar space is located between glandular tissue and the great pectoral muscle. Normally, this space contains only adipose tissue. [2]

Normal lymph nodes can also be identified on mammograms. More often they are visualized on the medio-lateral oblique projection in the axillary region and in some cases in the mammary gland tissue itself. [4]

References:

1. Островерхов Г. Е., Бомаш Ю. М., Лубоцкий Д. Н. Оперативная хирургия и топографическая анатомия. – Издательство» Медицинское информационное агентство», 2015. – С. 736-736.

2. Корженкова Г. П. Комплексная рентгено-сонографическая диагностика заболеваний молочной железы. – Фирма Стром, 2004.

3. Терновой С. К. Лучевая маммология: руководство для врачей. – ГЭОТАР-Медиа, 2007.

4. Ikeda D., Miyake K. K. Breast imaging: the requisites. – Elsevier Health Sciences, 2016.

RADIOLOGY STUDY

Radiology Study is the journal publishes relevant scientific articles on radiology, radionuclide diagnostics, ultrasound diagnostics and interventional radiology, including endovascular technologies, as well as other relevant areas of medical imaging and radiotherapy.

The electronic format of the journal provides wide availability of the publication, consistently high quality of illustrative material, the ability to place DICOM files of your cases. Each issue of the journal contains articles from leading specialists in radiology.

Languages: English and Russian.

Publication frequency: 4 issues per year (quarterly).

The Journal is distributed free of charge. Available in Russia and all over the world.

The Editorial Board of Radiology Study supports the policy aimed at compliance with all principles of publishing ethics. The ethical rules and norms correspond to those adopted by the leading international scientific publishers.

All submitted materials are subject to mandatory double-blind peer review.

The certificate of registration of mass media: El no. FS77-74575 - 14 December 2018.

Address for correspondence: RS-journal@yandex.ru   All materials for publication in the journal are sent to this address.